VOLUME 16 NUMBER 4 / December 2012

JOURNAL OF THE KOREAN SOCIETY FOR INDUSTRIAL AND APPLIED MATHEMATICS

The Korean Society for Industrial and Applied Mathematics

ISSN 1226-9433(print)
ISSN 1229-0645(electronic)

The Korean Society for Industrial and Applied Mathematics

Volume 16, Number 4, December 2012

contents

SUBNORMAL WEIGHTED SHIFTS WHOSE MOMENT MEASURES HAVE POSITIVE MASS AT THE ORIGIN
MI RYEONG LEE AND KYUNG MI KIM 217

HIGH-ORDER POTENTIAL FLOW MODELS FOR HYDRODYNAMIC UNSTABLE INTERFACE
SUNG-IK SOHN 225

BLOW UP OF SOLUTIONS WITH POSITIVE INITIAL ENERGY FOR THE NONLOCAL SEMILINEAR HEAT EQUATION
ZHONG BO FANG AND LU SUN 235

CRITERION FOR BLOW-UP IN THE EULER EQUATIONS VIA CERTAIN PHYSICAL QUANTITIES
NAMKWON KIM 243

PATTERN FORMATION FOR A RATIO-DEPENDENT PREDATOR-PREY MODEL WITH CROSS DIFFUSION
M. SAMBATH AND K. BALACHANDRAN 249

RETRACTION NOTICE TO “THE RELATIONSHIP BETWEEN NONCOMMUTATIVE AND LORENTZVIOLATING PARAMETERS IN QUANTUM”
A. HEIDARI, F. GHORBANI AND M. GHORBANI 257

J. KSIAM Vol.16, No.4, 217–223, 2012

SUBNORMAL WEIGHTED SHIFTS WHOSE MOMENT MEASURES HAVE POSITIVE MASS AT THE ORIGIN

MI RYEONG LEE† AND KYUNG MI KIM

DEPARTMENT OF MATHEMATICS, KYUNGPOOK NATIONAL UNIVERSITY, DAEGU, 702-701 KOREA
E-mail address: leemr@knu.ac.kr; kkm907@hanmail.net

ABSTRACT. In this note we examine the effects on subnormality of adding a new weight or changing some weights for a given subnormal weighted shift. We consider a subnormal weighted shift with a positive point mass at the origin by means of continuous functions. Finally, we introduce some methods for evaluating point mass at the origin about moment measures associated with weighted shifts.

1. INTRODUCTION

Let $\mathcal{H}$ be a separable, infinite dimensional, complex Hilbert space and let $\mathcal{L}(\mathcal{H})$ denote the algebra of all bounded linear operators on $\mathcal{H}$. For an operator T in $\mathcal{L}(\mathcal{H})$, T is called *normal* if $T^*T = TT^*$ and *subnormal* if T has normal extension on some Hilbert space containing $\mathcal{H}$. Recall that, given a bounded sequence of positive real numbers $\alpha : \alpha_0, \alpha_1, \cdots$, the *weighted shift* W_α associated with a weight sequence α is an operator on $\ell^2(\mathbb{Z}_+)$ defined by $W_\alpha e_n := \alpha_n e_{n+1}$ for all $n \geq 0$, where $\{e_n\}_{n=0}^\infty$ is the orthonormal basis for ℓ^2. In particular, W_α is normal if and only if $\alpha_n = 0$ for all $(n \geq 0)$. And we note that for a subnormal weighted shift W_α with $\alpha_n = \alpha_{n+1}$ for some $n \in \mathbb{N} \cup \{0\}$, subnormality of W_α immediately forces the weight α to be flat, that is, $\alpha_1 = \alpha_2 = \cdots$ ([7]). So we may assume that the weight sequence $\alpha = \{\alpha_n\}_{n=0}^\infty$ for a subnormal weighted shift W_α satisfies a strictly positive sequence converging to 1 and $\alpha_n < \alpha_{n+1}$ $(n \geq 0)$ to escape the trivial case.

It is well known for a description of subnormality for weighted shifts, called Berger's Theorem ([3]) that W_α is subnormal if and only if there exists a Borel probability measure μ supported in $[0, \|W_\alpha\|^2]$ such that $\beta_n^2 = \int_{[0,\|W_\alpha\|^2]} t^n d\mu$ $(n \geq 0)$, where the moments of W_α are defined by $\beta_0 := 1$ and $\beta_n := \beta_{n-1}\alpha_{n-1}$ $(n \geq 1)$. In such case, we call the measure μ, *moment measure* for the subnormal shift W_α. Recall that a weighted shift with weights $\{\alpha_n\}_{n=0}^\infty$ has a *subnormal backward extension* if for some positive number α_{-1}, the weighted shift with

Received by the editors January 26 2012; Accepted November 19 2012.
2010 *Mathematics Subject Classification.* 47B20, 47B37, 44A60.
Key words and phrases. subnormal, weighted shift operator, moment measure.
The first author was supported by Basic Science Research Program through the National Research Foundation of Korea(NRF) funded by the Ministry of Education, Science and Technology(2010-0025830).
† Corresponding author.

weights $\{\alpha_{n-1}\}_{n=0}^{\infty}$ is subnormal (cf. [4], [5]). In [1], R. Curto proved that a backward extension of a subnormal weighted shift fails to be subnormal whenever the associated probability measure has a positive mass at the origin. In [4], Hoover-Jung-Lambert have studied relationship between a subnormal weighted shift and its corresponding moment measures.

This note consists of three sections. In Section 2, we construct a subnormal weighted shift and a Borel probability measure with a positive point mass using a continuous function satisfying some integration formula. In Section 3, we obtain some formulas to get the positive value at the origin of the moment measure of a subnormal weighted shift. And we give some methods and concrete examples for evaluating such point mass at the origin.

Some of calculations in Section 2 and 3 are obtained throughout computer experiments using software tool Mathematica [8].

2. Construction of subnormality

Before we begin our work, we introduce a criterion for subnormal extensions of weighted shifts.

Proposition 2.1. ([1]) *Let W_α be a weighted shift with a weight sequence $\alpha = \{\alpha_n\}_{n=0}^{\infty}$ whose restriction to the subspace spanned by $\{e_1, e_2, ...\}$ is subnormal with associated measure μ. Then W_α is subnormal if and only if*

$$\frac{1}{t} \in L^1(\mu) \text{ and } \alpha_0^2 \leq (\|\frac{1}{t}\|_{L^1(\mu)})^{-1}.$$

In particular, W_α is never subnormal when $\mu(\{0\}) > 0$.

Now we introduce some notations and terminology in [4]. For a weighted shift W_α with a weight sequence $\alpha = \{\alpha_n\}_{n=0}^{\infty}$, we denote $W_\alpha|_{\mathcal{P}_k}$ for the restriction of W_α to the subspace $\mathcal{P}_k := \vee_{i \geq k}\{e_i\}$. Consider a subnormal weighted shift W_α with a weight $\alpha = \{\alpha_n\}_{n=0}^{\infty}$ and the corresponding measure μ. We write ω for a probability moment measure with the restriction $W_\alpha|_{\mathcal{P}_1}$. Then there exists a real number a with $0 < a \leq 1$ such that $\mu = a\delta_0 + \omega$ and $\omega(\{0\}) = 0$, where δ_0 denotes the Kronecker function.

Let us fix an integer $N \geq 1$, and define the restriction sequence $\alpha(N)$ of α by $\alpha(N)$: $\alpha_N, \alpha_{N+1}, ...$ Then the corresponding weighted shift $W_{\alpha(N)}$ is unitarily equivalent to $W_\alpha|_{\mathcal{P}_N}$. Since this is the restriction of a subnormal operator to an invariant subspace, $W_{\alpha(N)}$ is itself a subnormal weighted shift (with norm 1). Let μ_N be its associated probability measure and write $\mu_N = a_N\delta_0 + w_N$. Then we can have that the following relationships for these measures ([4]):

$$t d\mu_N = \frac{t^{N+1}}{\beta_N^2} d\mu \qquad \text{and} \qquad dw_N = \frac{t^N}{\beta_N^2} d\mu = \frac{t^N}{\beta_N^2} dw. \tag{2.1}$$

Proposition 2.2. *Suppose that W_α is a subnormal weighted shift with a weight sequence $\alpha = \{\alpha_n\}_{n=0}^{\infty}$ and the associated measure μ. Let $\widehat{\alpha}(k, x) : x, \alpha_k, \alpha_{k+1}, \cdots$ be a weight sequence by prefixing a positive real variable x to the restriction sequence $\alpha(k)$ of α and let $W_{\widehat{\alpha}(k,x)}$ be an associated weighted shift with a weight $\widehat{\alpha}(k, x)$ ($k \geq 0$).*

(i) *For* $k = 0$, $W_{\alpha(0,x)}$ *is subnormal if and only if*

$$x \leq \frac{\alpha_0}{\sqrt{\omega([0,1])}},$$

where $\mu = a\delta_0 + \omega$ *with* $\omega(\{0\}) = 0$. *In particular, if* $\mu(\{0\}) = a > 0$, *then* $\omega([0,1]) = 1 - a$, *and so* $W_{\alpha(x)}$ *is subnormal if and only if*

$$0 < x \leq \frac{\alpha_0}{\sqrt{1-a}}.$$

(ii) *For* $k \geq 1$, $W_{\widehat{\alpha}(k,x)}$ *is subnormal if and only if there exists a Borel probability measure* $\mu_{(k;x)}$ *corresponding to* $W_{\widehat{\alpha}(k,x)}$ *such that*

$$d\mu_{(k;x)} = \left[1 - \left(\frac{x}{\alpha_{k-1}}\right)^2\right] d\delta_0 + \frac{x^2}{\beta_k^2} t^{k-1} d\mu.$$

Proof. (i) See [4, Theorem 3.3].

(ii) We show the existence of a Borel probability measure on $[0,1]$ for a backstep extension $W_{\widehat{\alpha}(k,x)}$ of restriction weighted shift $W_\alpha|_{\mathcal{P}_k}$ for $k \geq 1$. Suppose that $W_{\widehat{\alpha}(k,x)}$ is subnormal. Then there exists a probability measure $\widehat{\mu}_{(k;x)}$ on $[0,1]$ such that

$$x^2\alpha_k^2\alpha_{k+1}^2 \cdots \alpha_{k+n-2}^2 = \int_{[0,1]} t^n d\widehat{\mu}_{(k;x)}.$$

Using (2.1) and the definition of the sequence $\{\beta_n\}$, we can obtain that

$$\begin{aligned} x^2 \int_{[0,1]} t^n d\mu_k &= x^2 \int_0^1 t^{n-1} \frac{t^{k+1}}{\beta_k^2}\, d\mu \\ &= \frac{x^2}{\beta_k^2}\beta_{n+k}^2 = x^2\alpha_k^2 \cdots \alpha_{k+n-1}^2, \end{aligned}$$

which is equivalent to

$$t d\widehat{\mu}_{(k;x)} = x^2 d\mu_k.$$

Hence we have that

$$d\widehat{\mu}_{(k;x)} = \frac{x^2}{\beta_k^2} t^{k-1} d\mu + a_k d\delta_0$$

for some $0 \leq a_k < 1$. Also, we can obtain that

$$\widehat{\mu}_{(k;x)}([0,1]) = \frac{x^2}{\beta_k^2} \int_{(0,1]} t^{k-1} d\mu + a_k\delta_0(\{0\}) = 1$$

and by the definition of sequence β_k^2, we obtain that

$$\widehat{\mu}_{(k;x)}(\sigma) = \frac{x^2}{\beta_k^2} \cdot \mu(\sigma) + \left(1 - \frac{x^2}{\alpha_{k-1}^2}\right) \delta_0(\sigma)$$

for any Borel subset σ in $[0,1]$. □

Until now we have discussed a point mass at the origin from the given subnormal weighted shift. Conversely from the given a point mass, we now discuss a subnormal weighted shift via a continuous function on $[0,1]$ using a integration formula below.

Theorem 2.3. *For $0 < a < 1$, let φ be a continuous function on $[0,1]$ with $\varphi(0) = 0$ and $\varphi(t) \geq 0$ on $(0,1]$ such that*

$$\int_0^1 \varphi(t)dt = 1 - a.$$

Then there exists a sequence $\alpha := \{\alpha_n\}_{n=0}^{\infty}$ such that the corresponding weighted shift is subnormal whose associated measure μ on $[0,1]$ satisfies

$$d\mu = ad\delta_0 + \varphi dt.$$

Proof. First we define a sequence $\{\beta_n\}_{n=0}^{\infty}$ by

$$\beta_n := \begin{cases} 1 & \text{if } n = 0, \\ \sqrt{\int_0^1 t^n \varphi(t)dt} & \text{if } n \geq 1. \end{cases}$$

Define a measure μ on $[0,1]$ such that

$$\mu(\sigma) = a \cdot \delta_0(\sigma) + \int_\sigma \varphi(t)dt \tag{2.2}$$

for any Borel subset σ in $[0,1]$. Observe that, for $n \geq 1$, by (2.2) we have

$$\begin{aligned}\int_{[0,1]} t^n d\mu &= \int_{\{0\}} t^n d\mu + \int_{(0,1]} t^n d\mu = 0 + \int_{(0,1]} t^n \varphi(t)dt \\ &= \int_{[0,1]} t^n \varphi(t)dt = \beta_n^2.\end{aligned}$$

Hence, for all $n \geq 0$, we have $\beta_n^2 = \int_{[0,1]} t^n d\mu$. Since μ is a probability measure and $\{\beta_n\}_{n=0}^{\infty}$ is the moment sequence, the measure μ induces a subnormal weighted shift associated with the weight sequence $\left\{\frac{\beta_{n+1}}{\beta_n}\right\}_{n=0}^{\infty}$. □

Example 2.4. In Theorem 2.3, we consider $\varphi(t) = 6(1-a)(t - t^2)$ with $0 < a < 1$. Then we obtain the weight sequence $\alpha = \{\alpha_n\}_{n=0}^{\infty}$ for subnormality of weighted shift with

$$\alpha : \alpha_0 = \sqrt{\frac{1-a}{2}},\ \alpha_n = \sqrt{\frac{n+2}{n+4}} \quad (n \geq 1).$$

Indeed, for $n \geq 1$,

$$\beta_n^2 = \int_0^1 t^n \varphi(t)\ dt = \frac{6(1-a)}{(n+2)(n+3)}.$$

Put $\alpha_n = \frac{\beta_{n+1}}{\beta_n}$ for $n \geq 1$. Then $\alpha_n = \sqrt{\frac{n+2}{n+4}}$ $(n \geq 1)$. From $\alpha_0 = \beta_1 = \sqrt{\frac{1-a}{2}}$, we can have a weight sequence $\alpha = \{\alpha_n\}_{n=0}^{\infty}$ associated the subnormal weighted shift.

Example 2.5. In Theorem 2.3, if we take $\varphi(t) = \sin \frac{\pi}{2} t$ $(0 \le t \le 1)$ and define a sequence $\{\beta_n\}_{n=0}^{\infty}$ as

$$\beta_n^2 := \begin{cases} 1 & (n = 0), \\ \int_0^1 t^n \sin \frac{\pi}{2} t \, dt & (n \ge 1), \end{cases}$$

then we have $a = 1 - \frac{2}{\pi}$. Put $\alpha_n := \frac{\beta_{n+1}}{\beta_n}$ $(n \ge 0)$. Hence we may obtain easily a weight sequence $\alpha := \{\alpha_n\}_{n=0}^{\infty}$ with

$$\alpha_0 = \frac{\pi}{2},\ \alpha_1 = \sqrt{\frac{2(\pi - 2)}{\pi}},\ \alpha_2 = \sqrt{\frac{3(\pi^2 - 8)}{2\pi(\pi - 2)}},$$
$$\alpha_3 = 2\sqrt{\frac{48 - 24\pi + \pi^3}{3\pi(\pi^2 - 8)}},\ \alpha_4 = \frac{1}{2}\sqrt{\frac{5(384 - 48\pi^2 + \pi^4)}{\pi(\pi^3 - 24\pi + 48)}}, \ldots.$$

Moreover, the probability measure $d\mu = (1 - \frac{2}{\pi}) d\delta_0 + \sin \frac{\pi}{2} t \ dt$ on $[0, 1]$ determines the subnormality of the weighted shift W_α.

3. COMPUTATIONS OF POINT MASS AT THE ORIGIN

In this section, in order to compute the positivity of moment measure at the origin for a subnormal weighted shift, we introduce some fundamental formulas for evaluating point mass at the origin for the measure associated with a weighted shift.

Lemma 3.1. ([4]) *Let W_α be a subnormal weighted shift with a weight sequence α and a moment measure μ. Then*

$$\mu(\{0\}) = \lim_{k \to \infty} \sum_{j=0}^{k} (-1)^j \binom{k}{j} \beta_j^2 = \lim_{k \to \infty} \sum_{j=0}^{\infty} \frac{(-k)^j}{j!} \beta_j^2$$

where $\beta_0 = 1$ and $\beta_n^2 = \int_0^1 t^n d\mu$ $(n \ge 1)$.

If we use the notion of the incomplete gamma function $\Gamma(a, z) := \int_z^\infty t^{a-1} e^{-t} dt$, we can have the following simple result.

Lemma 3.2.

$$\lim_{n \to \infty} \Gamma(0, n) = \lim_{n \to \infty} \int_n^\infty \frac{1}{te^t} dt = 0.$$

Proof. For $1 \le n \le t$, we have that $0 < t^{-1} e^{-t} \le e^{-t}$. Using definitions of improper integrals, we have $\int_n^\infty e^{-t} dt = e^{-n}$. Hence

$$\lim_{n \to \infty} \int_n^\infty e^{-t} dt = 0.$$

This completes our result. □

Example 3.3. Consider a weight sequence $\alpha : \alpha_n = \sqrt{\frac{(n+1)(2^{n+2}-1)}{2(n+2)(2^{n+1}-1)}}$ $(n \geq 0)$. Let $d\mu = 2 \cdot \chi_{[\frac{1}{2},1]} dt$. Since

$$\beta_n^2 = \int_0^1 t^n d\mu = 2\int_{\frac{1}{2}}^1 t^n dt = \frac{2}{n+1}\left(1 - \frac{1}{2^{n+1}}\right),\ (n \geq 1)$$

and

$$\beta_0 = \int_0^1 d\mu = 1,$$

the weighted shift W_α is a subnormal with the associated measure μ. Let a weight sequence $\widehat{\alpha}(x)(\equiv \widehat{\alpha}(0,x)) :\ x, \alpha_0, \alpha_1, \alpha_2, ...$ be a backward extension of α. Hence $W_{\widehat{\alpha}(x)}$ is subnormal if and only if

$$x^2 \int_0^1 \frac{1}{t} d\mu = 2x^2 \int_{\frac{1}{2}}^1 \frac{1}{t} dt = 2x^2 \ln 2 \leq 1,$$

which is equivalent to $0 < x \leq \sqrt{\frac{1}{2\ln 2}}$. By Lemma 3.1, we obtain

$$\begin{aligned}\mu(\{0\}) &= 1 - \lim_{n\to\infty} \sum_{i=1}^n (-1)^{i+1} \binom{n}{i} \beta_i^2 \\ &= 1 - \lim_{n\to\infty} \frac{n+1-2^{-n}}{n+1} = 0.\end{aligned}$$

Now we consider α' $(\equiv \widehat{\alpha}(1, \alpha_0'))$ with $\alpha_0' = \sqrt{\frac{1}{4\ln 2}}$ and $\alpha_n' = \alpha_n$ $(n \geq 1)$. We recall that the associated moment sequence $\left\{{\beta_n'}^2\right\}_{n=0}^\infty$ is given by $\beta_0' = 1$ and $\beta_n' = \alpha_{n-1}' \cdot \beta_{n-1}'$ for $n \geq 1$. From the Proposition 2.2, we take an corresponding probability measure $\mu' := \mu_{(1;\alpha_0')}$ with $W_{\alpha'}$. By simple computations, we can have that for all $n \geq 1$,

$${\beta_n'}^2 = \frac{2^{n+1}-1}{2^n(n+1)3\ln 2} \leq \frac{2}{3(n+1)\ln 2}.$$

We use the binomial theorem for the calculation $\int_0^{1/2} (1-x)^n\, dx$, we can obtain

$$\sum_{i=1}^n (-1)^{i+1} \binom{n}{i} \left(\frac{2}{i+1} - \frac{2^{i+1}-1}{(i+1)2^i}\right) = \frac{2^n(n-1)+1}{(n+1)2^n} \geq 0 \text{ for } n \geq 1,$$

which deduces the following result:

$$\sum_{i=1}^n (-1)^{i+1} \binom{n}{i} {\beta_i'}^2 \leq \frac{2}{3\ln 2} \sum_{i=1}^n (-1)^{i+1} \binom{n}{i} \frac{1}{i+1} \tag{3.1}$$

for all $n \geq 1$. Also we calculate the value of $\int_0^1 (1-x)^n\, dx$ via the binomial theorem, we can obtain that

$$\frac{1}{2}\binom{n}{1} - \frac{1}{3}\binom{n}{2} + \cdots + (-1)^{n+1} \frac{1}{n+1}\binom{n}{n} = \frac{n}{n+1} \tag{3.2}$$

for all $n \geq 1$. To show the positivity of the point mass $\mu'(\{0\})$ in Lemma 3.1, using (3.1) and (3.2), we can have that

$$\begin{aligned}\mu'(\{0\}) &= \lim_{n\to\infty}\sum_{i=0}^{n}(-1)^i\binom{n}{i}\beta_i'^2 = 1-\lim_{n\to\infty}\sum_{i=1}^{n}(-1)^{i+1}\binom{n}{i}\beta_i'^2\\ &\geq 1-\lim_{n\to\infty}\frac{2n}{3(n+1)\ln 2}=\frac{3\ln 2-2}{3\ln 2},\end{aligned}$$

which guarantees that $\mu'(\{0\}) > 0$.

Example 3.4. For the weight sequence α in Example 3.3, if we consider $\alpha' \equiv \widehat{\alpha}(2, \alpha_0')$ with $\alpha_0' = \sqrt{\frac{1}{2\ln 2}}$ and $\alpha_n' = \alpha_{n+1}$ $(n \geq 1)$. And applying Lemma 3.1 and 3.2 with α' and we have the corresponding probability measure $\mu' \equiv \mu_{(2;\alpha_0')}$, we can have that

$$\begin{aligned}\mu'(\{0\}) &= \lim_{n\to\infty}\sum_{i=0}^{\infty}\frac{(-n)^i}{i!}\left(\beta_i'\right)^2\\ &= \frac{1}{\ln 2}\lim_{n\to\infty}\Big(\Gamma(0,\frac{n}{2})-\Gamma(0,n)\Big)=0.\end{aligned}$$

Now to show the positivity of the measure at the origin as in Example 3.3, we have to take a real number a satisfying $a > 2\ln 2$ for a new weight sequence $\alpha'' \equiv \widehat{\alpha}(2, a)$ with $\alpha_0'' = \sqrt{\frac{1}{a}}$ and $\alpha_n'' = \alpha_{n+1}$ $(n \geq 1)$ and use the similar methods in Example 3.3. We leave some computations to interested readers.

REFERENCES

[1] R. Curto, *Quadratically hyponormal weighted shifts* , Integral Equations and Operator Theory **13**(1990), 49-66.
[2] R. Curto and L. Fialkow, *Recursively generated weighted shifts and the subnormal completion problem, I*, Integral Equations and Operator Theory **17**(1993), 202-246.
[3] P. Halmos, *Ten problems in Hilbert space*, Bull. Amer. Math. Soc. **76**(1970), 887-933.
[4] T. Hoover, I. B. Jung and A. Lambert, *Moment sequences and backward extensions of subnormal weighted shifts*, J. Austral. Math. Soc. **73**(2002), 27-36.
[5] Z. Jabłonski, I. B. Jung and J. Stochel, *Backward extensions of hyperexpansive operators*, Studia Math. **173**(2006), 233-257.
[6] A. Lambert, *Subnormality and weighted shifts*, J. London Math. Soc. **14**(1976), 476-480.
[7] J. Stampfli, *Which weighted shifts are subnormal*, Pacific J. Math. **17**(1966), 367-379.
[8] Wolfram Research, Inc. *Mathematica, Version 8.0*, Wolfram Research Inc., Champaign, IL, 2010.

J. KSIAM Vol.16, No.4, 225–234, 2012

HIGH-ORDER POTENTIAL FLOW MODELS FOR HYDRODYNAMIC UNSTABLE INTERFACE

SUNG-IK SOHN

DEPARTMENT OF MATHEMATICS, GANGNEUNG-WONJU NATIONAL UNIVERSITY, GANGNEUNG, KOREA
E-mail address: sohnsi@gwnu.ac.kr

ABSTRACT. We present two high-order potential flow models for the evolution of the interface in the Rayleigh-Taylor instability in two dimensions. One is the source-flow model and the other is the Layzer-type model which is based on an analytic potential. The late-time asymptotic solution of the source-flow model for arbitrary density jump is obtained. The asymptotic bubble curvature is found to be independent to the density jump of the fluids. We also give the time-evolution solutions of the two models by integrating equations numerically. We show that the two high-order models give more accurate solutions for the bubble evolution than their low-order models, but the solution of the source-flow model agrees much better with the numerical solution than the Layzer model.

1. INTRODUCTION

Fluid mixing occurs frequently in basic science and engineering applications. When a heavy fluid is supported by a lighter fluid in a gravitational field, the interface between the fluids is unstable under small disturbances. This phenomenon is known as the Rayleigh-Taylor (RT) instability [1, 2]. The RT instability may occur whenever the density and pressure gradients are in opposite directions and plays important roles in many fields ranging from astrophysics to inertial confinement fusion [3]. To investigate dynamics of this instability, extensive researches have been conducted for last decades. For a review, see Sharp [3].

Small perturbations at the interface in the RT instability grow into nonlinear structures in the form of bubbles and spikes. (See Fig. 1.) A bubble (spike) is a portion of the light (heavy) fluid penetrating into the heavy (light) fluid. At late times, the bubble in the RT instability attains a constant velocity. Eventually, turbulent mixing caused by vortex structures around spikes breaks the ordered fluid motion.

The main purpose of this paper is to develop high-order models for the interface evolution in the single-mode RT instability. Theoretical models for comprehensive descriptions of the motion of the interface are the potential flow models proposed by Layzer [4] and Zufiria [5]. Both the Layzer and Zufiria models approximate the shape of the interface near the bubble (or

Received by the editors April 30 2012; Accepted October 5 2012.
2010 *Mathematics Subject Classification.* 76B07, 76E17.
Key words and phrases. Rayleigh-Taylor instability, potential-flow models, bubble evolution.

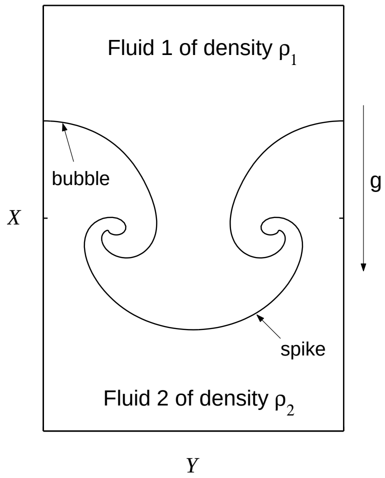

FIGURE 1. Flow description of RT instability. g represents the gravitational acceleration, and $\rho_1 > \rho_2$.

spike) tip as a parabola and give a set of ordinary differential equations to determine the position, velocity and curvature of the bubble (or spike). The main difference of the two models is that the velocity potential in the Layzer model is an analytical function of sinusoidal form, while in the Zufiria model, it has a point source (singularity). The Layzer and Zufiria models were limited to the case of infinite density ratio (fluid/vacuum) for a long time [6], but in the last decade there have been significant progresses in the models. Goncharov [7] and Sohn [8] generalized the Layzer model and the Zufiria model to the system of finite density jumps for the interface, respectively. Sohn [9, 10] also applied the Zufiria model to the multiple bubble interaction, and recently succeeded in the extension of the Layzer model to the unstable interfaces with surface tension and viscosity. Cao et al. [11] reported viscosity effects on the RT instability, by using the Zufiria model.

The potential flow models gave good predictions for the bubble velocity, but there were relatively large differences in the bubble curvature between the solutions of the models and numerical results. Moreover, the issue of the dependence of the bubble curvature on the density jump is not fully discovered yet. The bubble curvature is an important parameter because it sets a length scale and plays a key role in the dynamics of the bubble merger in the evolution of the initial multi-mode interface [9, 12]. In this paper, we present high-order solutions of the source-flow (Zufiria) model and the Layzer model to give quantitatively correct predictions for the bubble evolution.

In Section 2, we describe the high-order source-flow model for the motion of the interface of arbitrary density jump, and in Section 3, give the asymptotic solution of the bubble from the source-flow model. In Section 4, we present the high-order Layzer-model for the interface of infinite density ratio. Section 5 gives the time-evolution solutions of the bubble from the two high-order models, in comparisons with numerical results. Section 6 gives conclusions.

2. HIGH-ORDER SOURCE-FLOW MODEL

We consider an interface in a vertical channel filled with two fluids of different densities in two dimensions. The fluids are assumed as incompressible and inviscid. The densities of the upper (heavy) and lower (light) fluid are denoted as ρ_1 and ρ_2, respectively. From the assumption of the potential flow, there exist complex potentials $W_1(z) = \phi_1 + i\psi_1$ for the upper fluid and $W_2(z) = \phi_2 + i\psi_2$ for the lower fluid, where ϕ is the velocity potential and ψ the stream function. In the laboratory frame of reference, the location of the bubble tip is $Z(t) = X(t) + i\,Y(t)$ with $Y(t) = L/2$, where L is the channel width. The bubble moves in the x-direction with the tip velocity U. It is convenient to choose a frame of reference $(\hat{x}, \hat{y})$ moving together with the tip of the bubble. In other words, the frame of reference moves with the bubble velocity U. In this moving frame, the location of the bubble tip is $\hat{x} = \hat{y} = 0$ and the interface in the vicinity of the bubble tip can be written as

$$\eta(\hat{x}, \hat{y}, t) = \hat{x} + \sum_{j=1}^{\infty} \zeta_j(t)\, \hat{y}^{2j} = 0, \tag{2.1}$$

assuming the symmetry of the bubble. We here take the approximation of the interface (2.1) up to fourth-order in $\hat{y}$. The bubble curvature is denoted as $\xi = 2\zeta_1$.

The evolution of the bubble is determined by the kinematic condition and the Bernoulli equation

$$\frac{D\eta(\hat{x}, \hat{y}, t)}{Dt} = u + \sum_{j=1}^{\infty} \left(\frac{d\zeta_j}{dt} \hat{y}^{2j} + 2j\, \zeta_j\, \hat{y}^{2j-1} v \right) = 0, \tag{2.2}$$

$$\rho_1 \left[\frac{\partial \phi_1}{\partial t} + \frac{1}{2} |\nabla \phi_1|^2 + \left(g + \frac{dU}{dt} \right) \hat{x} \right] = \rho_2 \left[\frac{\partial \phi_2}{\partial t} + \frac{1}{2} |\nabla \phi_2|^2 + \left(g + \frac{dU}{dt} \right) \hat{x} \right], \tag{2.3}$$

where u and v are $\hat{x}$ and $\hat{y}$ components of the interface velocity, and g is the gravitational acceleration. The kinematic condition implies the continuity of the normal component of the fluid velocity across the interface.

The complex potentials of the fluids in the source-flow model [8, 9] are taken as

$$W_1(\hat{z}) = Q_1 \log \left[1 - e^{-k(\hat{z}+H)} \right] - U\hat{z}, \tag{2.4}$$

$$W_2(\hat{z}) = Q_2 \log \left[1 - e^{-k(\hat{z}-H)} \right] + (K - U)\hat{z}, \tag{2.5}$$

where $k = 2\pi/L$ is the wave number. Expanding the potentials (2.4) and (2.5) in powers of $\hat{z}$, and using the relation $dW_i/d\hat{z} = u - iv,\ i = 1, 2$, one can obtain the expressions for the interface velocity taken from the upper and lower fluids. Substituting these expressions into the kinematic condition (2.2), and satisfying up to the fourth-order in $\hat{y}$, we have

$$U = c_1 Q_1 = \tilde{c}_1 Q_2 + K, \tag{2.6}$$

$$\frac{d\zeta_1}{dt} = Q_1 \left(3c_2\zeta_1 + \frac{c_3}{2} \right) = Q_2 \left(3\tilde{c}_2\zeta_1 + \frac{\tilde{c}_3}{2} \right), \tag{2.7}$$

$$\frac{d\zeta_2}{dt} = Q_1\left(5c_2\zeta_2 - \frac{5}{2}c_3\zeta_1^2 - \frac{5}{6}c_4\zeta_1 - \frac{c_5}{24}\right)$$
$$= Q_2\left(5\tilde{c}_2\zeta_2 - \frac{5}{2}\tilde{c}_3\zeta_1^2 - \frac{5}{6}\tilde{c}_4\zeta_1 - \frac{\tilde{c}_5}{24}\right). \quad (2.8)$$

The second and fourth order equations in $\hat{y}$ of Eq. (2.3) are

$$\left(c_1\zeta_1 + \frac{c_2}{2}\right)\frac{dQ_1}{dt} + Q_1\left(c_2\zeta_1 + \frac{c_3}{2}\right)\frac{dH}{dt} - \frac{1}{2}Q_1^2c_2^2 + g\zeta_1$$
$$= r\left[\left(\tilde{c}_1\zeta_1 + \frac{\tilde{c}_2}{2}\right)\frac{dQ_2}{dt} + \frac{dK}{dt} - Q_2\left(\tilde{c}_2\zeta_1 + \frac{\tilde{c}_3}{2}\right)\frac{dH}{dt} - \frac{1}{2}Q_2^2\tilde{c}_2^2 + g\zeta_1\right], \quad (2.9)$$

$$\left(\frac{c_2}{2}\zeta_1^2 + \frac{c_3}{2}\zeta_1 + \frac{c_4}{24} - c_1\zeta_2\right)\frac{dQ_1}{dt} + Q_1\left(\frac{c_3}{2}\zeta_1^2 + \frac{c_4}{2}\zeta_1 + \frac{c_5}{24} - c_2\zeta_2\right)\frac{dH}{dt} + G_1$$
$$= r\left[\left(\frac{\tilde{c}_2}{2}\zeta_1^2 + \frac{\tilde{c}_3}{2}\zeta_1 + \frac{\tilde{c}_4}{24} - \tilde{c}_1\zeta_2\right)\frac{dQ_2}{dt}\right.$$
$$\left. - Q_2\left(\frac{\tilde{c}_3}{2}\zeta_1^2 + \frac{\tilde{c}_4}{2}\zeta_1 + \frac{\tilde{c}_5}{24} - \tilde{c}_2\zeta_2\right)\frac{dH}{dt} + G_2\right], \quad (2.10)$$

where

$$G_1 = \frac{Q_1^2}{2}\left(c_2^2\zeta_1^2 - 2c_2c_3\zeta_1 + \frac{c_3^2}{4} - \frac{c_2c_4}{3}\right) + g\zeta_2,$$
$$G_2 = \frac{Q_2^2}{2}\left(\tilde{c}_2^2\zeta_1^2 - 2\tilde{c}_2\tilde{c}_3\zeta_1 + \frac{\tilde{c}_3^2}{4} - \frac{\tilde{c}_2\tilde{c}_4}{3}\right) + g\zeta_2,$$

and $r = \rho_2/\rho_1$ denotes the density ratio. Here, the expressions for c_i are

$$c_1 = \frac{k}{e^{kH} - 1}, \qquad c_2 = -\frac{k^2e^{kH}}{(e^{kH} - 1)^2}, \qquad c_3 = \frac{k^3e^{kH}(e^{kH} + 1)}{(e^{kH} - 1)^3},$$
$$c_4 = -\frac{k^4e^{kH}(e^{2kH} + 4e^{kH} + 1)}{(e^{kH} - 1)^4}, \qquad c_5 = \frac{k^5e^{kH}(e^{3kH} + 11e^{2kH} + 11e^{kH} + 1)}{(e^{kH} - 1)^5}.$$

and $\tilde{c}_i(H) = c_i(-H)$. Equations (2.6)-(2.10) determine the dynamics of the bubble of finite density contrast. Note that Eq. (2.8) is a new equation from the low order model [8], and Eqs. (2.6)-(2.10) are the same as the low order model, except the terms with ζ_2 in Eq. (2.10).

One can check that Eqs. (2.6)-(2.10) remain the same even after retaining higher-order terms than the fourth order in $\hat{y}$, and thus expansions higher than the fourth order are not needed in this model. Usually, in other models, including the Layzer model, a higher-order expansion contributes a corresponding correction to the bubble motion. This is a crucial difference of the source-flow model from other theoretical models, and it explains why the high-order source-flow model is found to provide an accurate solution for the bubble motion.

3. ASYMPTOTIC SOLUTION OF SOURCE-FLOW MODEL

We now find the asymptotic solution for the bubble motion from the higher-order source-flow model. The system of the ordinary differential equations (2.6)-(2.10) has a critical point which corresponds to a steady rising bubble. The critical point (or, asymptotic solution) can be easily obtained by setting all the time derivatives of the variables to zero in Eqs. (2.7)-(2.10). The high-order asymptotic solution for the RT bubble is

$$\zeta_1 \to \frac{k(\lambda+1)}{6(\lambda-1)}, \qquad \zeta_2 \to \frac{k^3(\lambda^3+\lambda^2+\lambda+1)}{180(\lambda-1)^3},$$
$$H \to \frac{1}{k}\,\log\lambda, \qquad Q_1 \to \sqrt{\frac{2(\lambda+1)(\lambda-1)^3 Ag}{3\,\lambda\,(1+A)k^3}}, \tag{3.1}$$
$$U \to \frac{\sqrt{\lambda^2-1}}{\lambda}\sqrt{\frac{2Ag}{3(1+A)k}}, \qquad Q_2 \to 0, \qquad K \to U.$$

Here, A is the Atwood number, defined as $A = (\rho_1 - \rho_2)/(\rho_1 + \rho_2)$, and $\lambda = e^{kH(t\to\infty)} = (20 + 3\sqrt{39})/7$, which is the root, larger than 1, of the polynomial $p(\lambda) = 7\lambda^2 - 40\lambda + 7$. Therefore, from Eq. (3.1), the asymptotic bubble velocity is $0.984\sqrt{2Ag/(3(1+A)k)}$, and the asymptotic bubble curvature is $0.480k$, which is independent to the density jump. Note that the asymptotic solution of the low-order source-flow model [8] is $0.964\sqrt{2Ag/(3(1+A)k)}$ for the bubble velocity and $0.577k$ for the bubble curvature. Therefore, the correction factors of the high-order solution to the low-order solution are $U^{\text{high}}/U^{\text{low}} = 1.02$ for the velocity, and $\xi_1^{\text{high}}/\xi_1^{\text{low}} = 0.83$ for the curvature.

4. HIGH-ORDER LAYZER MODEL

We present the high-order Layzer model for the case of $A = 1$. For the Layzer model, we take the laboratory frame of reference. In this frame, the interface around the bubble tip can be approximated by

$$x = \eta(y,t) = \sum_{j=0}^{\infty} \zeta_j(t)\, y^{2j}. \tag{4.1}$$

Then, ζ_0 represents the longitudinal position of the bubble tip, and $d\zeta_0/dt$ is the velocity of the bubble tip. We give a general form of the velocity potential in the Layzer-type model by

$$\phi(x,y,t) = \sum_{\substack{j=1 \\ j:\ odd}}^{\infty} a_j(t)\,\cos(jky)\,e^{-jkx}. \tag{4.2}$$

The evolution of the bubble is again governed by the kinematic condition and the Bernoulli equation. In the case of $A = 1$, the right hand side of the Bernoulli equation (2.3) is set to zero.

One may apply the similar procedure as Section 2, to derive high-order equations. Satisfying the kinematic condition up to the fourth-order in y, we obtain the following equations

$$\frac{d\zeta_0}{dt} = -k \sum j a_j \, e^{-jk\zeta_0}, \tag{4.3}$$

$$\frac{d\zeta_1}{dt} = k^2 \sum j^2 \left(3\zeta_1 + \frac{1}{2} jk\right) a_j \, e^{-jk\zeta_0}, \tag{4.4}$$

$$\frac{d\zeta_2}{dt} = k^2 \sum j^2 \left(5\zeta_2 - \frac{5}{2} jk\zeta_1^2 - \frac{5}{6} j^2 k^2 \zeta_1 - \frac{1}{24} j^3 k^3\right) a_j \, e^{-jk\zeta_0}, \tag{4.5}$$

where all the summations are taken for $j = 1$ and 3. The second and fourth order equations from the Bernoulli equation are given by

$$\begin{aligned} k \sum j \left(\zeta_1 + \frac{1}{2} jk\right) e^{-jk\zeta_0} \frac{da_j}{dt} &= \frac{1}{2} k^4 \left(\sum j^2 a_j e^{-jk\zeta_0}\right)^2 \\ &\quad - k^3 \left(\sum j a_j e^{-jk\zeta_0}\right) \left[\sum j^2 a_j \left(\zeta_1 + \frac{1}{2} jk\right) e^{-jk\zeta_0}\right] + g\zeta_1, \end{aligned} \tag{4.6}$$

$$\begin{aligned} & k \sum j \left(\zeta_2 - \frac{1}{2} jk\zeta_1^2 - \frac{1}{2} j^2 k^2 \zeta_1 - \frac{1}{24} j^3 k^3\right) e^{-jk\zeta_0} \frac{da_j}{dt} \\ = \; & \frac{1}{2} k^4 \left[\sum j^2 \left(\zeta_1 + \frac{1}{2} jk\right) a_j e^{-jk\zeta_0}\right]^2 \\ & + k^3 \left(\sum j a_j e^{-jk\zeta_0}\right) \left[\sum j^2 \left(-\zeta_2 + \frac{1}{2} jk\zeta_1^2 + \frac{1}{2} j^2 k^2 \zeta_1 + \frac{1}{24} j^3 k^3\right) a_j e^{-jk\zeta_0}\right] \\ & - k^5 \left(\sum j^2 a_j e^{-jk\zeta_0}\right) \left[\sum j^3 \left(\zeta_1 + \frac{1}{6} jk\right) a_j e^{-jk\zeta_0}\right]^2 + g\zeta_2. \end{aligned} \tag{4.7}$$

Equations (4.3)-(4.7) determine the evolution of the bubble of infinite density ratio. In fact, it is possible to develop a high-order Layzer model for the case of finite density jump, but we have found that the equations in that model are quite coupled, and it is difficult to solve them.

5. COMPARISONS OF THE MODELS

We now examine the agreement of the models by comparing the finite-time solutions of the models with numerical results, for two cases of the Atwood number. The time-evolution solution of the source-flow model can be obtained by solving Eqs. (2.6)-(2.10) numerically. Differentiating Eqs. (2.6) and (2.7), dQ_2/dt and dK/dt in Eqs. (2.9) and (2.10) can be expressed in terms of dQ_1/dt, dH/dt, and other variables, Then, Eqs. (2.9) and (2.10) become the ordinary differential equations of dQ_1/dt and dH/dt, so that they can be integrated. For numerical integrations, we employ the standard fourth-order Runge-Kutta method. On the

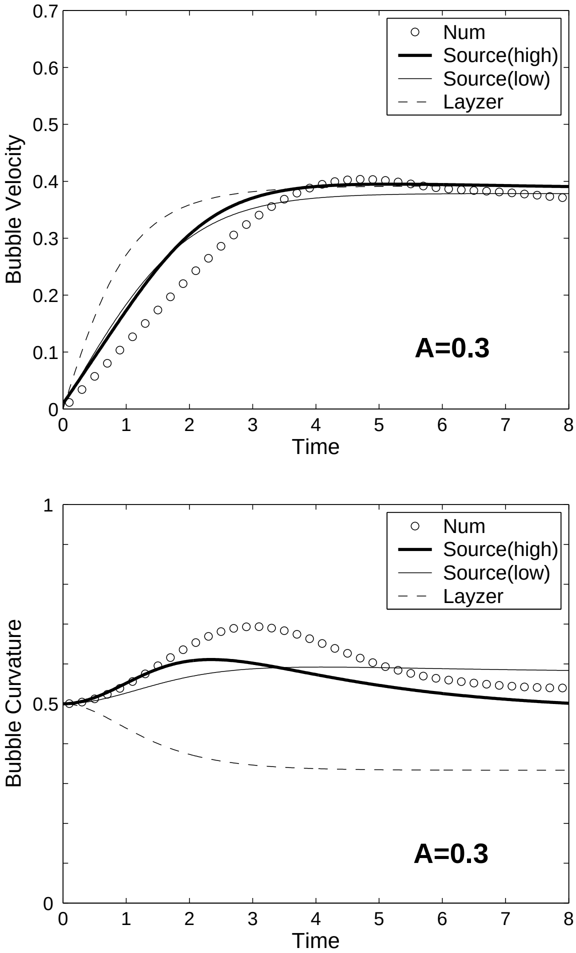

FIGURE 2. Bubble velocity and curvature for $A = 0.3$ from the low- and high-order source-flow models, the low-order Layzer model, and the numerical result.

other hand, the solution of the Layzer model can be obtained by integrating Eqs. (4.3)-(4.7) without any difficulty, because only da_1/dt and da_3/dt in Eqs. (4.6) and (4.7) are coupled.

In Figure 2, we compare the solutions for the bubble velocity and curvature of the RT instability for $A = 0.3$ from the low- and high-order source-flow model, and the low-order Layzer model [7] with the numerical result taken from Sohn [13]. The units in Fig. 2 (and also Fig. 3) are dimensionless. The dimensionless velocity, curvature and time are defined by $U\sqrt{k/g}$, ζ_1/k and $t\sqrt{kg}$, respectively. The numerical simulations in [13] are performed by the point vortex method based on the vortex sheet model. Note that the point vortex method has a regularization parameter for the finite density jump cases, which yields smoothing effects on

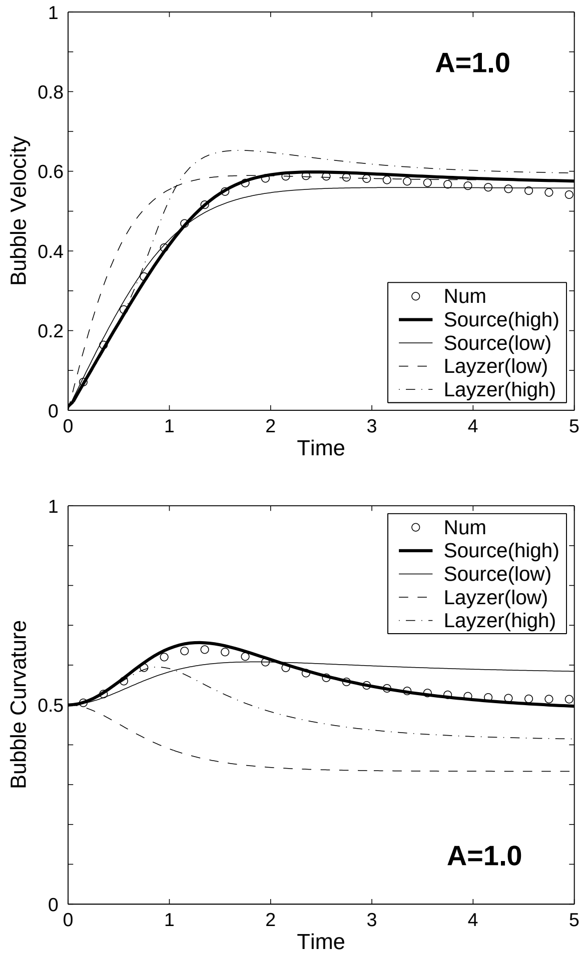

FIGURE 3. Bubble velocity and curvature for $A = 1$ from the low- and high-order source-flow models, the low- and high-order Layzer model, and the numerical result.

the solution. The physical parameters are set to $g = 1$ cm/s^2 and $k = 1$ cm^{-1}, and the initial amplitude of the interface is 0.5 cm. Figure 2 shows that the low-order source-flow model provides a good prediction for the bubble velocity, but not for the bubble curvature. The high-order solution of the source-flow model for the bubble curvature fits fairly well with the numerical solution. The growth of the bubble curvature at the early nonlinear stage is explained by the higher-order model. The Layzer model also gives a good prediction for the bubble velocity at the late time, but not at the early time. The bubble curvature from the Layzer model is quite different from the numerical result.

Figure 3 plots the solutions for the velocity and curvature of the RT bubble for $A = 1$ from the low- and high-order source-flow models, the low- and high-order Layzer models, and the numerical result. Figure 3 shows that the solution of the high-order source-flow model is in excellent agreements for both the bubble velocity and the curvature. This result indicates that the agreement of the source-flow model with the numerical result is better for larger density jump. We also find that for the bubble velocity, the solutions of the source-flow models again fit better than the Layzer models. The prediction for the bubble curvature from the low-order Layzer model is much improved by the higher-order model, but the difference with the numerical solution is still fairly large. This implies that some contributions from even higher-order variables are neglected in the model. To reduce the difference, equations higher than the fourth-order are required, but it is a formidable task.

6. CONCLUSIONS

We have presented the high-order solutions for the bubble evolution in the RT instability from the singular and analytic potential-flow models. The high-order source-flow model gives good predictions for both the bubble velocity and the curvature in the RT instability, over all times. The results presented in the paper validates that the source-type potential provides an appropriate description for the evolution of the unstable interface.

We have found the limitations of the Layzer model. In order to give quantitative predictions for the bubble, the Layzer model requires even higher-order expansions, while the present source-flow model has all the fourth-order contributions, We presented the high-order Layzer model only for the case of the infinite density ratio. Even if one finds a procedure of the numerical integration for the high-order Layzer model for the finite density jumps, it seems to be not promising.

The asymptotic bubble curvature of the RT instability is shown to be independent to the Atwood number. This behavior of the RT bubble is consistent with results of full numerical simulations for the Euler equation [14]. It is also contrasted with the bubble curvature of the Richtmyer-Meshkkov instability [15], which is a shock-accelerated interfacial instability. In the Richtmyer-Meshkkov instability, it has been known that the asymptotic bubble curvature is dependent on the density jump [8].

The present models may not be directly applicable to the spike evolution, except the cases of $A \approx 1$. It is because for a finite density jump, the mushroom-like vortex structure is pronounced around the spike, which makes increase of the drag, and therefore this effect should be considered in the modeling. So far, no model for the spike evolution of the finite density jump has been established. Extension of the present models to the spike would be an interesting and challenging subject.

ACKNOWLEDGMENTS

This research was supported by Basic Science Research Program through the National Research Foundation of Korea (NRF) funded by the Ministry of Education, Science and Technology (Grant No. 2012-0002995).

REFERENCES

[1] Lord Rayleigh, *Investigation of the character of the equilibrium of an incompressible heavy fluid of variable density*, Proc. London Math. Soc. **14** (1883), 170–177.

[2] G. I. Taylor, *The instability of liquid surfaces when accelerated in a direction perpendicular to their planes I*, Proc. R. Soc. London A **201** (1950), 192–196.

[3] D. Sharp, *An overview of Rayleigh-Taylor instability*, Physica D **12** (1984), 3–10.

[4] D. Layzer, *On the instability of superimposed fluids in a gravitational field*, Astrophys. J. **122** (1955), 1–12.

[5] J. Zufiria, *Bubble competition in Rayleigh-Taylor instability*, Phys. Fluids **31** (1988), 440–446.

[6] J. Hecht, U. Alon and D. Shvarts, *Potential flow models of Rayleigh-Taylor and Richtmyer-Meshkov bubble fronts*, Phys. Fluids **6** (1994), 4019–4030.

[7] V. N. Goncharov, *Analytic model of nonlinear, single-mode, classical Rayleigh-Taylor instability at arbitrary Atwood numbers*, Phys. Rev. Lett. **88** (2002), 134502: 1–4.

[8] S.-I. Sohn, *Density dependence of a Zufiria-type model for Rayleigh-Taylor and Richtmyer-Meshkov bubble fronts*, Phys. Rev. E **70** (2004), 045301: 1–4.

[9] S.-I. Sohn, *Bubble interaction model for hydrodynamic unstable mixing*, Phys. Rev. E **70** (2007), 066312: 1–12.

[10] S.-I. Sohn, *Effects of surface tension and viscosity on the growth rates of Rayleigh-Taylor and Richtmyer-Meshkov instabilities*, Phys. Rev. E **80** (2009), 055302: 1–4.

[11] Y. G. Cao, H. Z. Guo, Z. F. Zhang, Z. H. Sun and W. K. Chow, *Effects of viscosity on the growth of Rayleigh-Taylor instability*, J. Phys. A: Math. Theor. **44** (2011), 275501: 1–8.

[12] B. Cheng, J. Glimm and D. H. Sharp, *A three-dimensional renormalization group bubble merger model for Rayleigh-Taylor mixing*, Chaos **12** (2002), 267–274.

[13] S.-I. Sohn, *Vortex model and simulations for Rayleigh-Taylor and Richtmyer-Meshkov instabilities*, Phys. Rev. E **69** (2004), 036703: 1–11.

[14] P. Ramaprabhu and G. Dimonte, *Single-mode dynamics of the Rayleigh-Taylor instability at any density ratio*, Phys. Rev. E **71** (2005), 036314: 1–9.

[15] R. D. Richtmyer, *Taylor instability in shock acceleration of compressible fluids*, Commun. Pure Appl. Math. **13** (1960), 297–319.

J. KSIAM Vol.16, No.4, 235–242, 2012

BLOW UP OF SOLUTIONS WITH POSITIVE INITIAL ENERGY FOR THE NONLOCAL SEMILINEAR HEAT EQUATION

ZHONG BO FANG† AND LU SUN

SCHOOL OF MATHEMATICAL SCIENCES, OCEAN UNIVERSITY OF CHINA, QINGDAO 266100, P.R. CHINA
E-mail address: fangzb7777@hotmail.com

ABSTRACT. In this paper, we investigate a nonlocal semilinear heat equation with homogeneous Dirichlet boundary condition in a bounded domain, and prove that there exist solutions with positive initial energy that blow up in finite time.

1. INTRODUCTION

In this paper, we consider the initial Dirichlet-boundary problem for nonlocal semilinear heat equation

$$u_t - \Delta u + \int_0^t g(t-s)\Delta u(x,s)ds = f(u), \quad x \in \Omega, t > 0, \tag{1.1}$$

$$u(x,t) = 0, \quad x \in \partial\Omega, t > 0, \tag{1.2}$$

with the initial condition

$$u(x,0) = u_0(x) \in L^\infty(\Omega) \cap W_0^{1,2}(\Omega), \quad x \in \Omega. \tag{1.3}$$

where $\Omega \subset \mathbb{R}^N (N \geq 1)$ is a bounded domain with sufficient smooth boundary, relaxation function $g : R^+ \to R^+$ is a bounded C^1 function and nonlinearity $f(u) \in C(R)$.

Equation (1.1) arises naturally from a variety of mathematical models in engineering and physical science. For example, in the study of heat conduction in materials with memory term, the classical Fourier's law of heat flux is replaced by the following form:

$$q = -d\nabla u - \int_{-\infty}^t \nabla[k(x,t)u(x,\tau)]d\tau, \tag{1.4}$$

where u, d and the integral term represent temperature, diffusion coefficient, and the effect of memory term in the material, respectively. The study of this type of equations has drawn a considerable attention, see [1-5]. In mathematical view, one would expect the integral term in the equation to be dominated by the leading term. Therefore, one can apply the theory of parabolic equations to this type of equations.

Received by the editors August 8 2012; Accepted December 24 2012.
2010 *Mathematics Subject Classification.* 35K65, 35K20, 35A70.
Key words and phrases. nonlocal semilinear heat equation, blow-up, positive initial energy .
† Corresponding author. Tel.: +86 0532 66787153; fax: +86 0532 66787211.

When $g = 0$ and the nonlinearity is in the form of power function in equation (1.1), problem (1.1)-(1.3) has been studied by various authors and several results concerning global and non-global existence have been established. For instance, in the early 1970s, Levine [6] introduced concavity method and showed that solutions with negative energy blow up in finite time. Later, this method was improved by Kalantarov et al. [7] to more general situations. Other studies about equations with gradient term in bounded or unbounded domains, we refer to [8,9]. In addition, for quasilinear equations, there are some results about the influence of initial energy on blow-up solutions of initial boundary value problem as well. For instance, Zhao [10] established a nonglobal existence result of blow-up solutions with initial energy satisfying

$$E(0) = \frac{1}{p}\int_\Omega |\nabla u_0(x)|^p dx - \int_\Omega F(u_0(x))dx \le -\frac{4(p-1)}{pT(p-2)^2}\int_\Omega u_0^2(x)dx,$$

which was generalized by Levine et al. [11]. Existence results of blow-up solutions with nonpositive and positive initial energy, one can see [12,13]. Lately, Messaoudi [14] studied problem (1.1)-(1.3) when there is a memory term (i.e.$g \neq 0$) and the nonlinearity is in the form of power function. He established a blow-up result when initial energy is nonpositive. For more results about relations between energy and blow-up solutions to nonlocal hyperbolic equation, we refer to [15] and references therein.

In the works mentioned above, most problems were supposed that the initial energy is negative or non-positive to ensure the occurrence of blow-up. But to our knowledge, there are few works about the influence of positive initial energy on blow-up solutions of parabolic equation. The aim of this paper is to find sufficient condition of existence of blow-up solutions with positive initial energy when the fully nonlinear term $f(u)$ and relaxation function g satisfy some proper conditions.

In order to show our result, we assume that $f \in C(R)$, $F(u) = \int_0^u f(s)ds$, and

$$\inf\{\int_\Omega F(u)dx : |u| = 1\} > 0. \tag{1.5}$$

Denote by C_* the optimal constant of Sobolev embedding inequality

$$(\int_\Omega F(u)dx)^{\frac{1}{r}} \le C_*\|\nabla u\|_2, u \in W_0^{1,2}(\Omega), \tag{1.6}$$

where $r \in (2, \frac{2N}{N-2}]$ is a fixed constant, that is

$$C_*^{-1} = \inf_{u\in W_0^{1,2}(\Omega), u\neq 0} \frac{\|u\|_2}{(\int_\Omega F(u)dx)^{\frac{1}{r}}}.$$

For relaxation function g, we assume that

$$g(s) \ge 0,\ g'(s) \le 0,\ 1 - \int_0^\infty g(s)ds = l > 0. \tag{1.7}$$

We also set

$$\alpha = B^{-\frac{r}{r-2}},\ E_1 = (\frac{1}{2} - \frac{1}{r})B^{-\frac{2r}{r-2}} = (\frac{1}{2} - \frac{1}{r})\alpha^2. \tag{1.8}$$

where $B = C_*/l$.

Our main result is as follows:

Theorem 1.1. *Let $f \in C(R)$ satisfy condition (1.5)(1.6) and*

$$sf(s) \geq rF(s) \geq |s|^r,\ r > 2. \tag{1.9}$$

For g, we let it satisfy (1.7) and

$$\int_0^\infty g(s)ds < \frac{1 - c_0}{1 - \frac{3}{4}c_0}, \tag{1.10}$$

where $c_0 = \frac{1+(r-2)(\alpha_1/\alpha_2)^r}{r} < 1$. If the initial datum is chosen to ensure that

$$E(0) < E_1 \tag{1.11}$$

and

$$\|\nabla u_0\|_2 > \alpha_1, \tag{1.12}$$

then the strong solution u blows up in finite time.

Remark 1.2. *Our result improves the results of Messaoudi [14].*

2. THE PROOF OF THEOREM 1.1

In order to prove Theorem 1.1, we first introduce the "modified" energy functional

$$E(t) = \frac{1}{2}(g \circ \nabla u)(t) + \frac{1}{2}(1 - \int_0^\infty g(s)ds)\|\nabla u(t)\|_2^2 - \int_\Omega F(u)dx, \tag{2.1}$$

where

$$(g \circ v)(t) = \int_0^t g(t-s)\|v(t) - v(s)\|_2^2 ds. \tag{2.2}$$

Multiplying (1.1) with $-u_t$ and integrating over Ω, after some manipulations (see [15]), we get

$$-\frac{d}{dt}E(t) = -\int_0^t g'(t-s)\int_\Omega \frac{1}{2}|\nabla u(s)-\nabla u(t)|^2 dxds + g(t)\int_\Omega \frac{1}{2}|\nabla u(t)|^2 dx + \int_\Omega |u_t|^2 dx \geq 0,$$

for regular solutions, from which we can deduce that

$$\frac{d}{dt}E(t) \leq 0.$$

The same result can be established for almost every t by simple density argument.

Similar to [16], we give a definition for a strong solution of (1.1)-(1.3).

Definition A strong solution of (1.1)-(1.3) is a function $u \in C([0,T); H_0^1(\Omega)) \cap C^1([0,T); L^2(\Omega))$, satisfying $\frac{d}{dt}E(t) \leq 0$ and

$$\int_0^t \int_\Omega (\nabla u \cdot \nabla \phi - \int_0^s \nabla u(\tau) \cdot \nabla \phi(s) d\tau + u_t \phi - f(u)\phi) dxds = 0$$

for all $t \in [0,T)$ and all $\phi \in C([0,T); H_0^1(\Omega))$.

Remark 2.1. *The condition* $1-\int_0^\infty g(s)ds = l > 0$ *is necessary to guarantee the parabolicity of system (1.1)-(1.3).*

We prove the following two lemmas by using the idea of Vitillaro in [17].

Lemma 2.2. *Suppose that* u *is a strong solution of (1.1)-(1.3), and* $E(0) < E_1$, $\|\nabla u_0\|_2 > \alpha_1$, *then there exists a positive constant* $\alpha_2 > \alpha_1$, *so that*

$$[(1-\int_0^\infty g(s)ds)\|\nabla u\|_2^2 + (g\circ\nabla u)(t)]^{\frac{1}{2}} \geq \alpha_2, \tag{2.3}$$

$$(\int_\Omega rF(u)dx)^{\frac{1}{r}} \geq B\alpha_2. \tag{2.4}$$

Proof. First, by (1.6), we can get

$$\begin{aligned} E(t) &= \frac{1}{2}(g\circ\nabla u)(t) + \frac{1}{2}(1-\int_0^t g(s)ds)\|\nabla u\|_2^2 - \int_\Omega F(u)dx \\ &\geq \frac{1}{2}(g\circ\nabla u)(t) + \frac{1}{2}(1-\int_0^t g(s)ds)\|\nabla u\|_2^2 - \frac{1}{r}B^r\|\nabla u\|_2^r \\ &\geq \frac{1}{2}(g\circ\nabla u)(t) + \frac{1}{2}(1-\int_0^t g(s)ds)\|\nabla u\|_2^2 \\ &\quad -\frac{1}{r}B^r[(1-\int_0^t g(s)ds)\|\nabla u\|_2^2 + (g\circ\nabla u)(t)]^{\frac{r}{2}} \\ &= \frac{1}{2}\zeta^2 - \frac{B^r}{r}\zeta^r \doteq h(\zeta), \end{aligned} \tag{2.5}$$

where $\zeta = (1-\int_0^t g(s)ds)\|\nabla u\|_2^2 + (g\circ\nabla u)(t)$.

It is easy to see that h is increasing for $0 < \zeta < \alpha_1$ and decreasing for $\zeta > \alpha_1$; $h(\zeta) \to -\infty$ as $\zeta \to +\infty$ and $h(\alpha_1) = E_1$, where α_1 and E_1 are constants defined in (1.8). Since $E(0) < E_1$, $\|\nabla u_0\|_2 > \alpha_1$, we can know that there exists a constant $\alpha_2 > \alpha_1$ such that $E(0) = h(\alpha_2)$. Then by (2.5), we have $h(\|\nabla u_0\|_2) < E(0) = h(\alpha_2)$, which implies that $\|\nabla u_0\|_2 \geq \alpha_2$.

To establish (2.3), we assume that there exists a $t_0 > 0$ such that

$$[(1-\int_0^{t_0} g(s)ds)\|\nabla u\|_2^2 + (g\circ\nabla u)(t_0)]^{\frac{1}{2}} < \alpha_2.$$

Because of the continuity of $(1-\int_0^t g(s)ds)\|\nabla u\|_2^2 + (g\circ\nabla u)(t)$, we can choose t_0 such that

$$[(1-\int_0^{t_0} g(s)ds)\|\nabla u\|_2^2 + (g\circ\nabla u)(t_0)]^{\frac{1}{2}} > \alpha_1.$$

And from (2.5), we get

$$E(t_0) \geq h([(1-\int_0^{t_0} g(s)ds)\|\nabla u\|_2^2 + (g\circ\nabla u)(t_0)]^{\frac{1}{2}}) > h(\alpha_2) = E(0),$$

which is impossible according to Lemma 1, then (2.3) is established.

It follows from (2.1) that

$$\begin{aligned}\int_\Omega F(u)dx &\geq \frac{1}{2}(g\circ\nabla u)(t)+\frac{1}{2}(1-\int_0^t g(s)ds)\|\nabla u\|_2^2-E(0)\\ &\geq \frac{1}{2}\alpha_2^2-h(\alpha_2)=\frac{B^r}{r}\alpha_2^r,\end{aligned}$$

from which we can draw inequality (2.4), then the proof is complete. □

Setting

$$H(t)=E_1-E(t),\ t\geq 0, \tag{2.6}$$

we have the following Lemma:

Lemma 2.3. *Suppose that $E(0)<E_1$, then for all $t\geq 0$,*

$$0<H(0)\leq H(t)\leq \int_\Omega F(u)dx. \tag{2.7}$$

Proof. By $\frac{d}{dt}E(t)\leq 0$, we have

$$\frac{d}{dt}H(t)\geq 0,$$

and thus

$$H(t)\geq H(0)=E_1-E(0)>0,\ t\geq 0.$$

From (2.1) and (2.6), we have

$$H(t)=E_1-\frac{1}{2}(g\circ\nabla u)(t)-\frac{1}{2}(1-\int_0^t g(s)ds)\|\nabla u\|_2^2+\int_\Omega F(u)dx.$$

From (2.3) and (2.5), we then obtain that

$$\begin{aligned}&E_1-\frac{1}{2}[(1-\int_0^t g(s)ds)\|\nabla u\|_2^2+(g\circ\nabla u)(t)]\\ &\leq E_1-\frac{1}{2}\alpha_2^2\leq E_1-\frac{1}{2}\alpha_1^2=-\frac{1}{r}\alpha_1^2<0,\ \forall t\geq 0,\end{aligned}$$

which guarantees $H(t)\leq\int_\Omega F(u)dx$. The proof is complete. □

Proof of Theorem 1.1 We define $L(t)=\frac{1}{2}\int_\Omega u^2(x,t)dx$ and differentiate L to get

$$\begin{aligned}L'(t)&=\int_\Omega uu_t dx\\ &=\int_\Omega u(\Delta u-\int_0^t g(t-s)\Delta u(x,s)ds+f(u)]dx\\ &=-\int_\Omega|\nabla u|^2dx+\int_0^t g(t-s)\int_\Omega\nabla u(x,t)\cdot\nabla u(x,s)dxds+\int_\Omega uf(u)dx\\ &=-\int_\Omega|\nabla u|^2dx+\int_0^t g(t-s)\int_\Omega\nabla u(x,t)\cdot[\nabla u(x,s)-\nabla u(x,t)]\end{aligned}$$

$$\geq -\int_\Omega |\nabla u|^2 dx - \int_0^t g(t-s)\int_\Omega |\nabla u(x,t)\cdot[\nabla u(x,s)-\nabla u(x,t)]|$$

$$+\int_0^t g(t-s)\|\nabla u(x,t)\|_2^2 ds + r\int_\Omega F(u)dx. \tag{2.8}$$

By using Schwartz inequality, we have,

$$L'(t) \geq r\int_\Omega F(u)dx - (1-\int_0^t g(s)ds)\|\nabla u\|_2^2$$

$$-\int_0^t g(t-s)\|\nabla u(x,t)\|_2\|\nabla u(x,s)-\nabla u(x,t)\|_2 ds, \tag{2.9}$$

Then by using Young inequality to the last term, we get

$$L'(t) \geq r\int_\Omega F(u)dx - (1-\frac{3}{4}\int_0^t g(s)ds)\|\nabla u(x,t)\|_2^2 - (g\circ\nabla u)(t). \tag{2.10}$$

Next from (2.9), we deduce that

$$\|\nabla u(x,t)\|_2^2 = \frac{1}{1-\int_0^t g(s)ds}[2E(t)-(g\circ\nabla u)(t)+2\int_\Omega F(u)dx]$$

. Substitute into (2.10), we arrive at

$$L'(t) \geq r\int_\Omega F(u)dx - 2\frac{1-\frac{3}{4}\int_0^t g(s)ds}{1-\int_0^t g(s)ds}E(t) + \frac{1-\frac{3}{4}\int_0^t g(s)ds}{1-\int_0^t g(s)ds}(g\circ\nabla u)(t)$$

$$-2\frac{1-\frac{3}{4}\int_0^t g(s)ds}{1-\int_0^t g(s)ds}\int_\Omega F(u)dx - (g\circ\nabla u)(t)$$

$$= r\int_\Omega F(u)dx + 2\frac{1-\frac{3}{4}\int_0^t g(s)ds}{1-\int_0^t g(s)ds}(H(t)-E_1)$$

$$+[\frac{1-\frac{3}{4}\int_0^t g(s)ds}{1-\int_0^t g(s)ds}-1](g\circ\nabla u)(t) - 2\frac{1-\frac{3}{4}\int_0^t g(s)ds}{1-\int_0^t g(s)ds}\int_\Omega F(u)dx. \tag{2.11}$$

By combining (2.4) and Lemma 2.2, we get that

$$L'(t) \geq 2\frac{1-\frac{3}{4}\int_0^t g(s)ds}{1-\int_0^t g(s)ds}H(t) + [\frac{1-\frac{3}{4}\int_0^t g(s)ds}{1-\int_0^t g(s)ds}-1](g\circ\nabla u)(t)$$

$$+[r-2\frac{1-\frac{3}{4}\int_0^t g(s)ds}{1-\int_0^t g(s)ds}]\int_\Omega F(u)dx - 2\frac{1-\frac{3}{4}\int_0^t g(s)ds}{1-\int_0^t g(s)ds}\frac{r-2}{2r}\frac{\alpha_1^r}{\alpha_2^r}B^r\alpha_2^r$$

$$\geq \gamma H(t) + C_0\int_\Omega F(u)dx, \tag{2.12}$$

where

$$\gamma = 2\frac{1-\frac{3}{4}\int_0^t g(s)ds}{1-\int_0^t g(s)ds} > 0,$$

$$\begin{aligned} C_0 &= r - 2\frac{1-\frac{3}{4}\int_0^t g(s)ds}{1-\int_0^t g(s)ds} - (r-2)\frac{\alpha_1^r}{\alpha_2^r}\frac{1-\frac{3}{4}\int_0^t g(s)ds}{1-\int_0^t g(s)ds} \\ &= r - [2 + (r-2)\frac{\alpha_1^r}{\alpha_2^r}]\frac{1-\frac{3}{4}\int_0^t g(s)ds}{1-\int_0^t g(s)ds} > 0, \end{aligned}$$

because of $r > 2,\ \alpha_2 > \alpha_1$.

Next we use Hölder inequality to estimate $L^{\frac{r}{2}}(t)$:

$$L^{\frac{r}{2}}(t) \le C\|u\|_r^r \le Cr\int_\Omega F(u)dx, \tag{2.13}$$

then from (2.12), (2.13) and Lemma 2.3, we arrive at

$$L'(t) \ge \beta L^{\frac{r}{2}}(t),\ \beta = \frac{C_0}{Cr}. \tag{2.14}$$

A direct integration of (2.14) from 0 to t yields

$$L^{\frac{r}{2}-1}(t) \ge \frac{1}{L^{1-\frac{r}{2}}(0) - (\frac{r}{2}-1)\beta t}, \tag{2.15}$$

Then $L(t)$ blows up at a finite time $t_* \le \frac{L^{1-\frac{r}{2}(0)}}{(\frac{r}{2}-1)\beta}$, and so does $u(x,t)$. The proof of Theorem 1.1 is complete.

ACKNOWLEDGMENTS

This work is supported by the Natural Science Foundation of Shandong Province of China(ZR 2012AM018).

REFERENCES

[1] G. Da Prato and M. Iannelli, Existence and regularity for a class of integro-differential equations of parabolic type, Math. Anal. Appl. 112(1)(1985)36-55.

[2] A. Friedman, Mathematics in Industrial Problems. Part 5, The IMA Volumes in Mathematics and Its Applications, vol. 49, Springer, New York, 1992.

[3] J. A. Nohel, Nonlinear Volterra equations for heat flow in materials with memory, Integral and Functional Differential Equations (Proc. Conf., West Virginia Univ., Morgantown, W. Va, 1979) (T. L. Herdman, H. W. Stech, and III S. M. Rankin, eds.), Lecture Notes in Pure and Appl. Math., Dekker, New York, 67(1981)3-82.

[4] H. M. Yin, On parabolic Volterra equations in several space dimensions, SIAM J. Math. Anal. 22(6)(1991)1723-1737.

[5] H. M. Yin, Weak and classical solutions of some nonlinear Volterra integrodifferential equations, Comm. Partial Differential Equations 17(7-8)(1992)1369-1385.

[6] H. A. Levine, Some nonexistence and instability theorems for solutions of formally parabolic equations of the form $Pu_t = -Au + F(u)$, Arch. Ration. Mech. Anal. 51(1973)371-386.

[7] V. K. Kalantarov, O. A. Ladyzhenskaya, The occurrence of collapse for quasilinear equations of parabolic and hyperbolic types, J. Sov. Math. 10(1978)53-70.
[8] J. Ball, Remarks on blow-up and nonexistence theorems for nonlinear evolution equations, Quart. J. Math. Oxford. 28(2)(1977)473-486.
[9] L. Alfonsi and F.Weissler, Blow up in R^n for a parabolic equation with a damping nonlinear gradient term, Nonlinear Diffusion Equations and Their Equilibrium States, 3 (Gregynog, 1989), Progr. Nonlinear Differential Equations Appl., vol. 7, Birkhauser Boston, Massachusetts, 1992, pp. 1-20.
[10] J. N. Zhao, Existence and nonexistence of solutions for $u_t = div(|\nabla u|^{p-2}\nabla u) + f(\nabla u, u, x, t)$, J. Math. Anal. Appl. 172(1)(1993)130-146.
[11] H. A. Levine, S. Park, and J. Serrin, Global existence and nonexistence theorems for quasilinear evolution equations of formally parabolic type, J. Differential Equations 142(1)(1998)212-229.
[12] S. A. Messaoudi, A note on blow up of solutions of a quasilinear heat equation with vanishing initial energy, J. Math. Anal. Appl. 273(1)(2002)243-247.
[13] W.J. Liu, M.X. Wang, Blow-up of the solution for a p-Laplacian equation with positive initial energy, Acta. Appl. Math. 103(2008) 141-146.
[14] S. A. Messaoudi, Blow-up of solutions of a semilinear heat equation with a Visco-elastic term, Progress in Nonlinear Differential Equations and Their Applications, 64(2005)351-356.
[15] S. A. Messaoudi, Blow-up of positive-initial-energy solutions of a nonlinear viscoelastic hyperbolic equation, J. Math. Anal. Appl. 320 (2006)902-915.
[16] P. Pucci, J. Serrin, Asymptotic stability for nonlinear parabolic systems, Energy Methods in Continuum Mechanics (Oviedo, 1994), Kluwer Academic Publishers, Dordrecht, (1996)66-74.
[17] E. Vitillaro, Global nonexistence theorems for a class of evolution equations with dissipation. Arch. Ration. Mech. Anal. 149(1999)155-182.

J. KSIAM Vol.16, No.4, 243–248, 2012

CRITERION FOR BLOW-UP IN THE EULER EQUATIONS VIA CERTAIN PHYSICAL QUANTITIES

NAMKWON KIM

DEPARTMENT OF MATHEMATICS, CHOSUN UNIVERSITY, KWANGJU, 501-759, REPUBLIC OF KOREA
E-mail address: kimnamkw@chosun.ac.kr

ABSTRACT. We consider the (possible) finite time blow-up of the smooth solutions of the 3D incompressible Euler equations in a smooth domain or in $\mathbf{R}^3$. We derive blow-up criteria in terms of L^∞ of the partial component of Hessian of the pressure together with partial component of the vorticity.

1. INTRODUCTION

Let Ω be $\mathbf{R}^3$ or a smooth bounded domain in $\mathbf{R}^3$. We consider the Euler equations of incompressible fluid in Ω:

$$\left\{ \begin{array}{c} u_t + (u \cdot \nabla)u + \nabla p = f, \\ \text{div} u = 0, \end{array} \right. \tag{1.1}$$

with initial velocity u_0 and boundary condition $u \cdot n = 0$. Here n is the unit outer normal vector to $\partial\Omega$.

It is known that if the initial velocity, $u_0 \in H^m$, $m > 5/2$, then there exists a unique smooth solution for the Euler equations up to some positive time(See [7], [10] and references therein). A natural question is then whether this solution quits to be smooth and thus quits to be a strong solution any more in a finite time. This question is also related with the regularity problem of the 3D incompressible Navier-Stokes equations[6]. There have been developed many criteria whether the solution blows up in a finite time. Especially, blow-up criteria in terms of vorticity, deformation tensor, and the Hessian of the pressure have been developed under various situations(See for example [2, 4, 5, 9] and [3]). Also, localization of these blow-up criteria have been developed[1, 8]. Among others, blow-up criteria by pressure involve all components of the Hessian of the pressure until now.

Our aim here is developing blow-up criteria in terms of L^∞ norm of some components of the Hessian of the pressure together with L^∞ norm of some component of the vorticity. We shall derive differential inequalities for L^q norm of vorticity using certain equations for the product

Received by the editors November 19 2012; Accepted December 7 2012.
2010 *Mathematics Subject Classification.* 35Q30, 35K15.
Key words and phrases. Euler equations, blow-up, criterion.
This work is partially supported by Chosun university, 2007.

of the vorticity and the deformation tensor and apply the energy argument to those inequalities. This approach is already used in [1] to derive a criterion by L^∞ norm of the Hessian of the pressure.

2. BLOW-UP CRITERIA

Let T^* be the blow-up time of a classical solution u for the Euler equations (1.1). The singular set for u at time $t = T^*$ is defined by the set of all $x \in \overline{\Omega}$ such that for any ball B centered at x,

$$\liminf_{t \nearrow T^*} \|u(t)\|_{H^m(B\cap\Omega)} = \infty.$$

Let us denote the singular set by S. It is clear that S is a closed set in $\overline{\Omega}$. If $H \subset S$ is a bounded closed component of S, we call it an isolated singular set for u. Trivially, $dist(H, S - H) > 0$.

Let $\omega = \nabla \times u$ be the vorticity and $J = \omega \cdot \nabla u$. Then, taking a curl to the first equation in (1.1) and by direct calculation, for $0 < t < T^*$

$$\frac{\partial \omega}{\partial t} + (u \cdot \nabla)\omega = J, \tag{2.1}$$

$$\frac{\partial J}{\partial t} + (u \cdot \nabla)J = -(\omega \cdot \nabla)\nabla p. \tag{2.2}$$

Throughout this section, we denote $\tilde{\omega} = (\omega_1, \omega_2)$ and $\tilde{\nabla} = (\partial_1, \partial_2)$. We start with the following lemma first.

Lemma 1. *Let $g \in C[0, a]$ and $A, B \in L^1[0, a]$ be nonnegative and*

$$g(t) - g(0) \le \int_0^t \int_0^s (A(\tau)g(\tau) + B(\tau))\, d\tau ds, \quad t \in [0, a]. \tag{2.3}$$

Then g satisfies

$$g(t) \le \left(g(0) + \int_0^t \int_0^s B\right) \exp \int_0^t \int_0^s A d\tau ds. \tag{2.4}$$

Proof. We shall show that for any $\epsilon > 0$,

$$g(t) \le \left(g(0) + \int_0^t \int_0^s B + \epsilon\right) \exp \int_0^t \int_0^s A(\tau) d\tau ds.$$

For simplicity, let us denote $X(s) = \exp \int_0^s \int_0^r A(\tau) d\tau dr$. Suppose not. Then, since the LHS of the above is smaller than the RHS of the above at $t = 0$, for some $\epsilon > 0$, there would be a first time $b < a$ such that the equality holds in the above. However, at $t = b$, by (2.3),

$$\begin{aligned} g(b) \le & \int_0^b \int_0^t A(s) \left[(g(0) + \epsilon)X(s) + X(s) \int_0^s \int_0^r B \right] \\ & + g(0) + \int_0^b \int_0^t B. \end{aligned}$$

By integration by parts,

$$\begin{aligned}\int_0^b\int_0^t A(s)X(s) &= \left[\int_0^t A(s)X(t) - \int_0^t\left(\int_0^s A(\tau)\right)^2 X(s)\right]\\ &\le \int_0^b\int_0^t A(s)X(t)\\ &= X(b)-X(0) = \exp\int_0^b\int_0^r A(\tau)d\tau dr - 1,\end{aligned}$$

Similarly, by integration by parts,

$$\begin{aligned}\int_0^t A(s)X(s)\int_0^s\int_0^r B = \int_0^t A(s)X(t)\int_0^t\int_0^r B\\ -\int_0^t\left(\int_0^s A(\tau)d\tau\right)^2 X(s)\int_0^s\int_0^r B\\ -\int_0^t\int_0^s A(\tau)d\tau X(s)\int_0^s B\\ \le \int_0^t A(s)X(t)\int_0^t\int_0^r B.\end{aligned}$$

Therefore,

$$\begin{aligned}\int_0^b\int_0^t A(s)X(s)\int_0^s\int_0^r B &\le \int_0^b\int_0^t A(s)X(t)\int_0^t\int_0^r B\\ &\le X(b)\int_0^b\int_0^r B - \int_0^b X(t)\int_0^t B\\ &\le X(b)\int_0^b\int_0^r B - \int_0^b\int_0^t B\end{aligned}$$

by $X(t)\ge 1$. Gathering these inequalities, we have

$$g(b)\le (g(0)+\epsilon)X(b)-\epsilon + X(b)\int_0^b\int_0^r B = g(b)-\epsilon.$$

Thus, we arrive at a contradiction and finish the proof. □

Theorem 1. *Let u be a smooth solution of (1.1), $f\in L^\infty(0,\infty;H^m)$ a external force, H be an isolated singular set. For any relatively open set G containing H,*

$$\int_0^{T^*}\left[(T^*-t)\|\nabla\partial_3 p(t)\|_{L^\infty(G)} + \sup_{s\le t}\|\tilde\omega\|_{L^\infty(G)}(s)\right]dt = +\infty.$$

Proof. Without loss of generality, we can assume that there exist an (relatively) open smooth set $W\supset G$, $dist(W^c,G)>0$. Let ξ be a smooth cutoff function such that $\xi=1$ on G and

$\xi = 0$ on W^c. For convenience, let us denote

$$A_3(t) = (\int_\Omega |\omega_3|^q \xi dx)^{1/q}, \quad B_3(t) = (\int_\Omega |J_3|^q \xi dx)^{1/q},$$

$\tilde{D} = \|\tilde{\nabla}\partial_3 p\|_{L^\infty(W)}$, and $D_3 = \|\partial_3^2 p\|_{L^\infty(W)}$. $\tilde{A}$ is similarly defined with $\tilde{\omega}$. Multiplying the third component of (2.1) by $\xi|\omega_3|^{q-2}\omega_3$ and integrating over Ω, we have

$$\begin{aligned}\frac{1}{q}\frac{d}{dt}\int_\Omega |\omega_3|^q \xi dx &= \frac{1}{q}\int_\Omega |\omega_3|^q (u\cdot\nabla)\xi dx + \int_\Omega |\omega_3|^{q-2}\omega_3 J_3 \xi dx \\ &\le \frac{C}{q}\int_{W_\Omega\setminus G_\Omega} |\omega|^q |u| dx + \int_\Omega |\omega_3|^{q-1}|J_3|\xi dx \\ &\le CC^{q+1}\frac{1}{q}\|u\|^{q+1}_{H^m(W_\Omega\setminus G_\Omega)} + A_3^{q-1}B_3. \end{aligned} \tag{2.5}$$

Similarly, multiplying (2.2) by $\xi|J_3|^{q-2}J_3$ and integrating over Ω, we have

$$\begin{aligned}\frac{1}{q}\frac{d}{dt}\int_\Omega |J_3|^q \xi dx &= \frac{1}{q}\int_\Omega |J_3|^q (u\cdot\nabla)\xi dx - \int_\Omega |J_3|^{q-2}J_3(\omega\cdot\nabla)\nabla_3 p\xi dx \\ &\le \frac{C}{q}\int_{W_\Omega\setminus G_\Omega} |J|^q|u|dx + \int_\Omega |J_3|^{q-1}[|\omega_3||\partial_3^2 p| + |\tilde{\omega}||\tilde{\nabla}\partial_3 p|]\xi dx \\ &\le \frac{C}{q}C^{2q+1}\|u\|^{2q+1}_{H^m(W_\Omega\setminus G_\Omega)} + \Big[\|\partial_3^2 p\|_{L^\infty(W_\Omega)}(\int_\Omega |\omega_3|^q\xi dx)^{\frac{1}{q}} \\ &+\tilde{A}\tilde{D}\Big](\int_\Omega |J_3|^q\xi dx)^{\frac{q-1}{q}} \\ &\le \frac{C^{2q+2}}{q} + D_3A_3B_3^{q-1} + \tilde{A}\tilde{D}B_3^{q-1}. \end{aligned} \tag{2.6}$$

From the above equation, we get

$$\begin{aligned}(B_3^q + C^{2q})^{\frac{q-1}{q}}\frac{d}{dt}(B_3^q + C^{2q})^{1/q} &= \frac{1}{q}\frac{d}{dt}B_3^q \\ &\le \frac{C^{2q+2}}{q} + D_3A_3B_3^{q-1} + \tilde{A}\tilde{D}B_3^{q-1} \\ &\le (\frac{C^2}{q} + D_3A_3 + \tilde{A}\tilde{D})(B_3^q + C^{2q})^{\frac{q-1}{q}}. \end{aligned}$$

Therefore, applying the Gronwall lemma, we have

$$(B_3^q + C^{2q})^{1/q}(t) \le (B_3^q + C^{2q})^{1/q}(0) + \int_0^t (\frac{C^2}{q} + D_3A_3 + \tilde{A}\tilde{D}). \tag{2.7}$$

Plugging the above into (2.5), we have

$$\frac{1}{q}\frac{d}{dt}A_3^q(t) \le \frac{1}{q}C^{2q+2} + A_3^{q-1}\left(C + \int_0^t \tilde{A}\tilde{D} + \int_0^t D_3A_3\right).$$

Then, we again have

$$\begin{aligned}(A_3^q + C^{2q})^{\frac{q-1}{q}} \frac{d}{dt}(A_3^q + C^{2q})^{\frac{1}{q}} &= \frac{1}{q}\frac{d}{dt}A_3^q \\ &\le \frac{C^{2q+2}}{q} + A_3^{q-1}\left(C + \int_0^t \tilde{A}\tilde{D} + \int_0^t D_3 A_3\right) \\ &\le \left(\frac{C^2}{q} + \int_0^t \tilde{A}\tilde{D} + \int_0^t D_3(A_3^q + C^{2q})^{1/q}\right) \times \\ &\quad (A_3^q + C^{2q})^{\frac{q-1}{q}}.\end{aligned}$$

Subsequently, by the Gronwall lemma,

$$(A_3^q + C^{2q})^{1/q}(t) \le (A_3^q + C^{2q})^{1/q}(0) + \int_0^t \int_0^s (\frac{C^2}{q} + D_3 A_3 + \tilde{A}\tilde{D}).$$

Here, we redefine C suitably large constant. C depends on u_0, T^*, and $\sup_t \|u\|_{H^m(W_\Omega \setminus G_\Omega)}(t)$ but can be chosen independent of q since $q > 1$. Integrating the above and using (2.4), we have

$$A_3(t) \le (C + A_3(0) + \int_0^t \int_0^s \tilde{A}\tilde{D}) \exp \int_0^t \int_0^s D_3.$$

Letting $q \to \infty$, we arrive at

$$\begin{aligned}\|\omega_3\|_{L^\infty(G)}(t) \le & (C + \|\omega_3\|_{L^\infty(W)}(0) + \int_0^t \int_0^s \|\tilde{\omega}\|_{L^\infty(W)} \|\tilde{\nabla}\nabla_3 p\|_{L^\infty(W)}) \times \\ & \exp \int_0^t \int_0^s \|\nabla_3^2 p\|_{L^\infty(W)}.\end{aligned}$$

Since $\nabla^2 p$ is also uniformly bounded on $W \setminus G$,

$$\int_0^t \int_0^s \|\tilde{\omega}\|_{L^\infty(W)} \|\tilde{\nabla}\nabla_3 p\|_{L^\infty(W)} \le \sup_{s<t} \|\tilde{\omega}\|_{L^\infty(W)}(s) \int_0^t \int_0^s \|\tilde{\nabla}\nabla_3 p\|_{L^\infty(W)},$$

and $\int_0^t \int_0^s h(\tau) d\tau = \int_0^t (t-s)h(s)$, we finish the proof by the local blow-up criterion by vorticity(see theorem 1 in [1]). □

Repeating the same argument in the proof of the above theorem, we have the following theorem.

Theorem 2. *Let u, f, H as in the previous theorem. For any relatively open set G containing H,*

$$\int_0^{T^*} \left[(T^* - t)\|\nabla\tilde{\nabla} p(t)\|_{L^\infty(G)} + \sup_{s \le t} \|\omega_3\|_{L^\infty(G)}(s)\right] dt = +\infty.$$

Proof. Multiplying (2.1) by $\xi|\tilde{\omega}|^{q-2}\tilde{\omega}$ and (2.2) by $\xi|\tilde{J}|^{q-2}\tilde{J}$ and integrating over Ω, we have

$$\frac{1}{q}\frac{d}{dt}\tilde{A}^q \le \frac{C^{2q+2}}{q} + \tilde{A}^{q-1}\tilde{B}.$$
$$\frac{1}{q}\frac{d}{dt}\tilde{B}^q \le \frac{C^{2q+2}}{q} + \tilde{D}A_3\tilde{B}^{q-1} + \tilde{A}\|\tilde{\nabla}^2 p\|_{L^\infty(W)}\tilde{B}^{q-1}.$$

Here, $\tilde{B} = (\int_\Omega |\tilde{J}|^q \xi dx)^{1/q}$ and A and D are as before. Following the same calculation as in the previous proof, we have

$$\tilde{A}(t) \le (C + \tilde{A}(0) + \int_0^t\int_0^s A_3\tilde{D}) \exp \int_0^t\int_0^s \|\tilde{\nabla}^2 p\|_{L^\infty(W)}.$$

Then, sending $q \to \infty$ again and using theorem 1 in [1], we arrive at the conclusion. □

Theorem 1 and 2 are different criteria from theorem 2 in [8] where blow-up criterion by stronger norm of $\tilde{\omega}$ was developed.

REFERENCES

[1] H. Bae, B. Jin, and N. Kim, On the localized blow-up of the 3D incompressible Euler equations, preprint, 2012

[2] Beale J T, Kato T and Majda A 1984, Remarks on the breakdown of smooth solutions for the 3-D Euler equations, Comm. Math. Phys. 94, no. 1, pp. 61-66().

[3] D. Chae, Incompressible Euler Equations: The Blow-up Problem and Related Results, in Handbook of Differential Equations: Evolutionary Equations, Elsevier, Volume 4, pp. 1-55, 2008.

[4] D.Chae, *On the finite-time singularities of the 3D incompressible Euler equations*, Comm.Pure.Appl.Math.Vol.LX, 0597-0617(2007).

[5] D. Chae, *Remarks on the blow-up criterion of the three-dimensional Euler equations,* Nonlinearity 18, no. 3, 1021-1029(2005).

[6] P. Constantin, *Note on loss of regularity for solutions of the 3-D incompressible Euler and related equations,* Comm. Math. Phys. 104, pp. 311-326(1986).

[7] T. Kato, *Nonstationary flows of viscous and ideal fluids in* **R**, J. Func. Anal., **9**, pp. 296-305(1972).

[8] N. Kim, *Remarks on the blow-up of solutions for the 3-D Euler equations*, Differential and Integral equations, 14, no.2,129-140(2001).

[9] G. Ponce, *Remarks on a paper: "Remarks on the breakdown of smooth solutions for the 3-D Euler equations" Comm. Math. Phys. 94, no. 1, 61-66(1984) by J. T. Beale, T. Kato and A. Majda.*, Comm. Math. Phys. 98, pp. 349-353 (1985).

[10] R. Temam, *On the Euler equations of incompressible perfect fluids*, J. Funct. Anal., 20(1975), pp. 32-43.

J. KSIAM Vol.16, No.4, 249–256, 2012

PATTERN FORMATION FOR A RATIO-DEPENDENT PREDATOR-PREY MODEL WITH CROSS DIFFUSION

M. SAMBATH† AND K. BALACHANDRAN

DEPARTMENT OF MATHEMATICS, BHARATHIAR UNIVERSITY, COIMBATORE 641 046, INDIA.
E-mail address: sambathbu2010@gmail.com, kb.maths.bu@gmail.com

ABSTRACT. In this work, we analyze the spatial patterns of a predator-prey system with cross diffusion. First we get the critical lines of Hopf and Turing bifurcations in a spatial domain by using mathematical theory. More specifically, the exact Turing region is given in a two parameter space. Our results reveal that cross diffusion can induce stationary patterns which may be useful in understanding the dynamics of the real ecosystems better.

1. INTRODUCTION

Beginning from the last century, numerous biological models have been received extensive attention. In particular, the predator-prey models have been of great interest to both applied mathematicians and ecologists. The first model to describe the size (density) dynamics of two populations interacting as a predator-prey system was developed independently by Alfred Lotka (1925) and Vito Volterra (1931). Since the classical Lotka-Volterra models suffer from some unavoidable limitations in describing precisely many realistic phenomena in biology, in some cases, they should make way to some more sophisticated models from both mathematical and biological points of view.

All the beings, including different kinds of populations, live in a spatial world and it is a natural phenomenon that a substance goes from high-density regions to low-density regions. As a result, more and more scholars use spatial model to study the interaction of the prey and predator [12]. Recently there has been considerable interest to investigate the stability behavior of a system of interacting populations by taking into account the effect of self as well as cross diffusion [14]. The term self diffusion implies the movement of individuals from a higher to lower concentration region. Cross diffusion expresses the population fluxes of one species due to the presence of the other species. The value of the cross diffusion coefficient may be positive, negative or zero. The positive cross diffusion coefficient denotes the movement of the species in the direction of lower concentration of another species and negative cross diffusion

Received by the editors September 27 2012; Accepted December 7 2012.
2010 *Mathematics Subject Classification.* 92D25, 70K50, 35B36.
Key words and phrases. Cross diffusion, Turing bifurcation, Predator-prey model, Pattern formation.
†Corresponding author.

coefficient denotes that one species tends to diffuse in the direction of higher concentration of another species [8].

In 1952, A.M. Turing first proposed the reaction-diffusion theory for pattern formation in his seminal work on the chemical basis of morphogenesis [21]. A fact in which a non-linear system is asymptotically stable in the absence of self and cross diffusions but unstable in the presence of self and cross diffusions is known as Turing instability. This concept has been playing significant roles in theoretical ecology, embryology and other branches of science. Similarly structured systems of ordinary differential equations govern the spatiotemporal dynamics of ecological population models, yet most of the simple models predict spatially homogeneous population distributions. One notable exception to this rule was demonstrated by Bartumeus et al. [1, 3] who reported that intra-predator interaction, or interference, may facilitate spatial pattern formation in a variation of the DeAngelis model [7, 15].

It has been observed that the spatially extended reaction-diffusion models for prey-predator interaction and various kinds of spatial patterns have been reported (see [4, 10, 18, 19]). A limited number of papers has appeared on resulting patterns exhibited by spatiotemporal prey-predator model with ratio-dependent functional response. Banerjee [2] performed the linear stability analysis for a diffusive predator-prey model with ratio-dependent functional response for the predator and reported the diffusion driven instability behavior and resulting Turing structures with heterogeneous environment. Earlier Fan and Li [9] studied the global asymptotic stability of the unique positive constant equilibrium solution for the same type of ratio-dependent prey-predator system with diffusion term. Recently Liu and Jin [13] analyze spatial pattern formation of a ratio-dependent predator-prey system with self diffusion. To the author's knowledge, the cross diffusion pattern generated by a ratio-dependent prey-predator model has not yet been reported by any researcher till date. The main objective of the present paper is to consider a two species prey-predator model with ratio-dependent functional response distributed over two-dimensional state space and establishes pattern formation for certain choices of initial population distribution.

Our paper is organized as follows. In Section 2, we analyze the predator-prey model with cross diffusion and derive the mathematical expressions for the Hopf and Turing bifurcation critical lines. In section 3, we present the result of pattern formation via numerical simulation. Finally we present some conclusion and discussion in section 4.

2. THE MODEL AND HOPF BIFURCATION ANALYSIS

The dynamics of ratio-dependent predator-prey system is governed by the following first order non-linear ordinary differential equations

$$\begin{cases} \dot{u}(t) = ru\left(1 - \dfrac{u}{K}\right) - \dfrac{\alpha uv}{(v + \alpha\beta u)}, \\ \dot{v}(t) = v\left(-\gamma + \dfrac{e\alpha u}{(v + \alpha\beta u)}\right), \\ u(t=0) = u_0 > 0, \quad v(t=0) = v_0 > 0, \end{cases} \tag{2.1}$$

where u and v are prey and predators, respectively. r represents intrinsic growth rate of the prey and carrying capacity K in the absence of predation, e conversion efficiency, α total attack rate for predator, β the handling time and γ death rate of the predator. The predator consumes the prey with the functional response known as Michaelis-Menten-Holling type functional response [11].

In order to minimize the number of parameters involved in the model, it is extremely useful to write the system in non-dimensionalized form. Thus we take

$$u \mapsto u/K, \quad v \mapsto v/K\alpha\beta \ \text{ and consider the dimensionless time } \ t \mapsto rt$$

and then we arrive at the equations of the following form,

$$\begin{cases} \dot{u}(t) = u\,(1-u) - \dfrac{auv}{(u+v)}, \\ \dot{v}(t) = c\left(-v + \dfrac{buv}{(u+v)}\right), \end{cases} \tag{2.2}$$

where $a = \alpha/r,\ b = e/\beta\gamma$ and $c = \gamma/r.$

Thus the model with cross diffusion becomes

$$\begin{cases} u_t = d_{11}\Delta u + d_{12}\Delta v + u\,(1-u) - \dfrac{auv}{(u+v)}, \\ v_t = d_{21}\Delta u + d_{22}\Delta v + c\left(-v + \dfrac{buv}{(u+v)}\right). \end{cases} \tag{2.3}$$

In the above, Δ is the Laplacian operator in two-dimensional space, $d_{11},\ d_{22}$ are self diffusion coefficients of prey and predator, $d_{12},\ d_{21}$ are the cross diffusion coefficients of prey and predator respectively.

The model (2.3) is analyzed with the initial populations $u(0) > 0,\ v(0) > 0.$
We also assume that no external input is imposed from outside. Hence the boundary condition are taken as

$$\left.\frac{\partial u}{\partial \nu}\right|_{(x,y)} = \left.\frac{\partial v}{\partial \nu}\right|_{(x,y)} = 0, \qquad (x,y) \in \partial\Omega,$$

where ν is the outward unit normal vector on $\partial\Omega$ and Ω is the two-dimensional spatial domain.

We are interested mostly in(from biological point of view) positive equilibrium point $E^* = (u^*, v^*)$, which corresponds to co-existence of prey and predator and is given by

$$u^* = \frac{a+b-ab}{b}, \qquad v^* = u^*(b-1). \tag{2.4}$$

It is easy to obtain the condition for ensuring that u^* and v^* are positive as $1 < b < a/(a-1),\ a > 1.$

We are interested in studying the stability behavior of the positive equilibrium point E^*. The Jacobian evaluated at the coexistence equilibrium $E^* = (u^*, v^*)$ is

$$J = \begin{pmatrix} a_{11} & a_{12} \\ a_{21} & a_{22} \end{pmatrix}. \tag{2.5}$$

where

$$a_{11} = a - \frac{a}{b^2} - 1, \quad a_{12} = -\frac{a}{b^2}, \quad a_{21} = \frac{(b-1)^2 c}{b}, \quad a_{22} = \left(\frac{1}{b} - 1\right) c.$$

We linearize the predator-prey system (2.3) around the spatially homogeneous fixed point (u^*, v^*) as follows:

$$\begin{pmatrix} u(\vec{\eta}, t) \\ v(\vec{\eta}, t) \end{pmatrix} = \begin{pmatrix} u^* \\ v^* \end{pmatrix} + \begin{pmatrix} \hat{u}(\eta, t) \\ \hat{v}(\eta, t) \end{pmatrix}, \tag{2.6}$$

where $|\hat{u}(\eta, t)| << u^*$, $|\hat{v}(\eta, t)| << v^*$ and $\vec{\eta}$ is in two-dimensional space.
By setting

$$\begin{pmatrix} u(\vec{\eta}, t) \\ v(\vec{\eta}, t) \end{pmatrix} = \begin{pmatrix} u_0 e^{\lambda t} e^{i\vec{k}, \hat{\eta}} \\ v_0 e^{\lambda t} e^{i\vec{k}, \hat{\eta}} \end{pmatrix}, \tag{2.7}$$

we obtain the characteristic equation

$$\left| J - \lambda I - k^2 D \right| = 0, \tag{2.8}$$

where

$$D = \begin{pmatrix} d_{11} & d_{12} \\ d_{21} & d_{22} \end{pmatrix}. \tag{2.9}$$

Now we obtain the characteristic polynomial from (2.8) as follows

$$\lambda^2 + T_k \lambda + D_k = 0, \tag{2.10}$$

where

$$T_k = (d_{11} + d_{22})k^2 - (a_{11} + a_{22}),$$

$$D_k = (d_{11}d_{22} - d_{12}d_{21})k^4 - (d_{11}a_{22} + d_{22}a_{11} - d_{12}a_{21} - d_{21}a_{12})k^2 + (a_{11}a_{22} - a_{12}a_{21}).$$

The roots of (2.10) are given by

$$\lambda_k = \frac{-T_k \pm \sqrt{T_k^2 - 4D_k}}{2}. \tag{2.11}$$

The onset of Hopf instability corresponds to the case when a pair of imaginary eigenvalues cross the real axis from the negative to positive side and this situation occurs only when the diffusion vanishes. Mathematically speaking, the Hopf bifurcation occurs when

$$Im(\lambda(k)) \neq 0, \quad Re(\lambda(k)) = 0 \text{ at } k = 0.$$

Then we get the critical value of the Hopf bifurcation parameter c, equal to c_H, where

$$c_H = \frac{a + b^2(1-a)}{b(1-b)}.$$

The positive equilibrium point (u^*, v^*) will be unstable if at least one of the roots of (2.10) is positive. By straight forward analysis, we find that D_k is a quadratic polynomial with respect to k^2. Its extremum is a minimum at some k^2 [17, 20]. From D_k, elementary differentiation with respect k^2 shows that

$$k_{min}^2 = \frac{d_{11}a_{22} + d_{22}a_{11} - d_{12}a_{21} - d_{21}a_{12}}{2\, det(D)}.$$

At the critical point, we have $D_k = 0$ when $k = k_{cr}$ [20]. For fixed kinetics parameters, this define a critical cross diffusion coefficient d_{12} as the root of equation

$$(d_{11}a_{22} + d_{22}a_{11} - d_{12}a_{21} - d_{21}a_{12})^2 - 4\, det(J)\, det(D) = 0.$$

The critical wavenumber k_{cr} is given by

$$k_{cr} = \sqrt{\frac{det(J)}{det(D)}}. \tag{2.12}$$

A general linear analysis [1, 5, 6] shows that the necessary conditions for yielding Turing patterns are given by

$$\begin{aligned}
&a_{11} + a_{22} < 0,\\
&a_{11}a_{22} - a_{12}a_{21} > 0,\\
&(d_{11}a_{22} + d_{22}a_{11} - d_{12}a_{21} - d_{21}a_{12}) > 0,\\
&(d_{11}a_{22} + d_{22}a_{11} - d_{12}a_{21} - d_{21}a_{12})^2 - 4\, det(J)\, det(D) > 0.
\end{aligned}$$

Mathematically speaking, the Turing bifurcation occurs when

$$Im(\lambda(k)) = 0, \quad Re(\lambda(k)) = 0 \text{ at } k = k_{cr} \neq 0.$$

and the wave number k_{cr} is the same as in (2.12). By direct calculation, we obtain the critical value of bifurcation parameter c, equal to c_T, where

$$\begin{aligned}
c_T \;=\; & \frac{1}{b^2(b-1)^2(d_{11} + (b-1)d_{12})^2}\\
& \Big(2\sqrt{b^3(b-1)^2(a + b(1-a))(a(d_{11} - d_{12}) + b^2 d_{12}(a-1))(d_{12} + d_{22}(b-1))(det(D))}\\
& + b(b-1)(a(d_{11} + (b-1)(2b+1)d_{12})d_{21} + a(b-1)^2(d_{12}(1+b) - d_{11})d_{22}\\
& + b^2(-2d_{12}d_{21} + (d_{11} + d_{12}(1-b))d_{22}))\Big),
\end{aligned}$$

where $det(J) = a_{11}a_{22} - a_{12}a_{21}$ and $det(D) = d_{11}d_{22} - d_{12}d_{21}$.

We fix the deterministic model values $a = 2.6,\ b = 1.6,\ d_{11} = 0.5,\ d_{21} = -0.1,\ d_{22} = 10$ and vary d_{12} as a function of c which is the coefficient of the cross diffusion of the prey. Now we discuss the bifurcations represented by these formulas in the parameter space. The bifurcation lines divide the parameter space into three distinct regions (see Fig. 1 (A)). The upper part of the displayed parameter space (where it is marked by III) corresponds to systems with homogeneous unconditionally stable equilibria. In region I, both Hopf and Turing bifurcations occur. The equilibria that can be found in the area, marked II, are stable with respect to homogeneous perturbations but lose their stability to homogeneous perturbations of specific wavenumber k.

Fig. 1 (B) shows the Turing space properly. The dispersion relation of the model (2.3) with several values of the one parameter fixed $c = 5$. It can be see from Fig. 1 (B) that when d_{12} increases, the available Turing models $[Re(\lambda) > 0]$ decrease and all available models are weakened.

3. Pattern formation

The dynamical behavior of the spatial predator-prey model cannot be determined by using analytical methods or normal forms. Thus we have to perform numerical simulations by computer. The main aim is to check whether a spatially homogeneous equilibrium is stable, unstable and to which solution to converges.

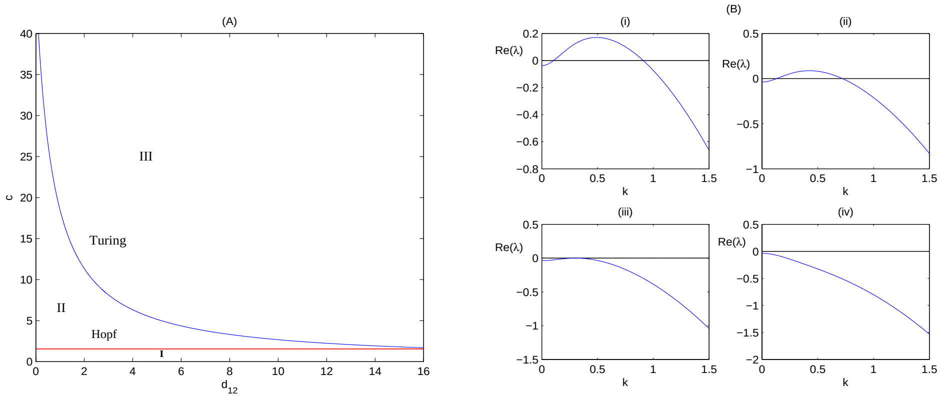

Fig.1 (A) The bifurcation diagram of model (2.3) with the parameter values $a = 2.6,\ b = 1.6,$ $d_{11} = 0.5,\ d_{21} = -0.1$ and $d_{22} = 10$. The red and blue lines correspond to the Hopf (c_H) and Turing (c_T) bifurcation critical lines respectively. The figure shows the Turing space (it is marked by II) with the area bounded by the Turing bifurcation line and the Hopf bifurcation line.
(B) Variation of dispersion relation of the model (2.3) with the parameter values $a = 2.6,\ b = 1.6,\ c = 5,\ d_{11} = 0.5,\ d_{21} = -0.1$ and $d_{22} = 10$. $(i)\ d_{12} = 0.5,\ \ (ii)\ d_{12} = 1.8,$ $(iii)\ d_{12} = 3.4$ (Turing instability occurs), $(iv)\ d_{12} = 7$ (Turing instability decays).

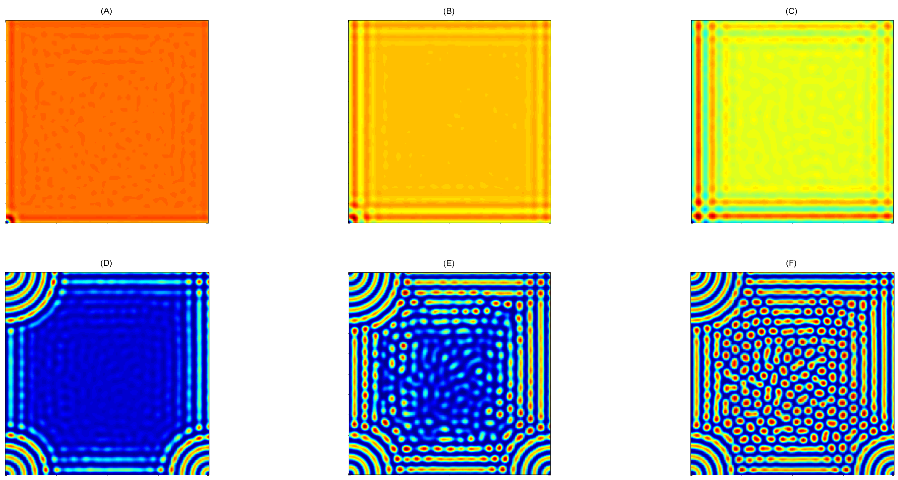

Fig. 2 Snapshots of contour of the time evolution of the prey at different instants with $a = 2.6,$ $b = 1.6,\ c = 5,\ d_{11} = 0.5,\ d_{21} = -0.1,\ d_{22} = 10$ and $d_{12} = 0.5$ and the parameter values in the Turing space. $(A)\ t = 0,\ (B)\ t = 100,\ (C)\ t = 250,\ (D)\ t = 350,\ (E)\ t = 500,\ (F)\ t = 1000.$

The problem defined by the reaction-diffusion system in two-dimensional space domain is solved in a discrete domain with $M \times N$ $(M = N = 200)$ lattice sites. The spacing in between the lattice points is defined by the lattice constants Δh. In the discrete system, the Laplacian describing diffusion is calculated using finite difference schemes, that is, the derivatives are approximated by differences over

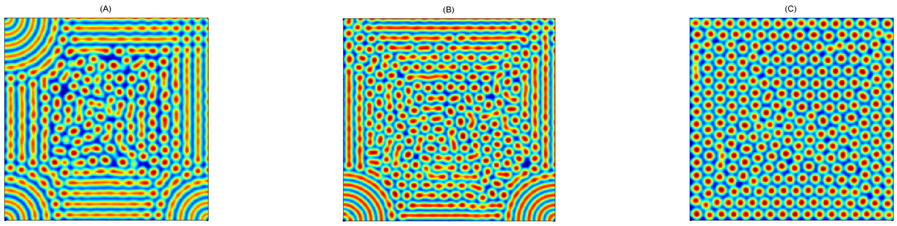

Fig. 3 Snapshots of contour of the prey at $t = 1000$ with $a = 2.6,\ b = 1.6,\ c = 5,\ d_{11} = 0.5$, $d_{21} = -0.1$ and $d_{22} = 10$. (A) $d_{12} = 1.5$, (B) $d_{12} = 3$, (C) $d_{12} = 7$. The parameters values are chosen values here in the Turing space.

Δh. For $\Delta h \to 0$ the differences approach the derivatives. The time evolution is also discrete, that is, the time goes by steps of Δt and it can be solved by using Euler's method. The model (2.3) is solved by numerically approximating the spatial derivatives and an explicit Euler's method for the time integration with a time step size of $\Delta t = 0.01$ and space step size $\Delta h = 0.1$. All our numerical simulations employ the non-zero initial conditions and the Neumann boundary conditions.

Fig. 2 shows the evolution of the spatial pattern of the prey at $t = 0,\ 100,\ 250,\ 350,\ 500,$ and 1000, with small random perturbation of the stationary solution u^* and v^* of the spatially homogeneous system with $d_{12} = 0.5$. In this case, one see that for the system (2.3) the random initial distribution leads to formation of irregular patterns. As the time is increased, spotted patterns and some striped patterns prevail over the whole domain finally and the dynamics of the system does not undergo any further change.

Fig. 3 (A) show the evolution of the spatial pattern of the prey at $t = 1000$ with small random perturbation of the stationary solution u^* and v^* of the spatially homogeneous system with $d_{12} = 1.5$. One can see from this figure that the strips-spots mixture patterns prevail in the whole domain.

Fig. 3 (B) show the evolution of the spatial pattern of the prey at $t = 1000$ with small random perturbation of the stationary solution u^* and v^* of the spatially homogeneous system with $d_{12} = 3$. One can see from this figure that the spots and labyrinth mixture patterns prevail in the whole domain.

As d_{12} increases to 7, we show the spatial pattern of prey at $t = 1000$ in Fig. $3(C)$. We see from the figure, the spotted patterns of spatial over the whole domain.

4. Conclusion

This article presents the pattern formation of a spatially extended ratio-dependent predator-prey model in two-dimensional space. Based on both mathematical analysis and numerical simulations, we find that its spatial pattern includes spotted patterns.

From the biological point of view, our results have some clear meaning. There has been a growing understanding, during the past years, regarding the dynamics of real ecosystems. It is important to reveal the different spatial dynamical regimes arising as a result of perturbation of the system parameters [10, 16]. The numerical simulation results indicate that the effect of the cross diffusion for pattern formation is remarkable. More specifically, as the value of predator cross diffusion coefficient d_{12} is increased, the spotted stripe-like and labyrinth patterns emerge (see Fig 2, 3). This enriches the dynamics of the effect of the cross diffusion of the predator-prey model.

REFERENCES

[1] D. Alonso, F. Bartumeus and J. Catalan, *Mutual interference between predators can give rise to Turing spatial patterns*, Ecology. **83** (2002), 28-34.

[2] M. Banerjee, *Self-replication of spatial patterns in a ratio-dependent predator-prey model*, Math. Comput. Modelling. **51** (2010), 44-52.

[3] F. Bartumeus, D. Alonso and J. Catalan, *Self-organized spatial structures in a ratio-dependent predator-prey model*, Physica A. **295** (2001), 53-57.

[4] D.L. Benson, J. Sherratt and P.K. Maini, *Diffusion driven instability in an inhomogeneous domain, Bull.Math.Biol.* **55** (1993), 365-384.

[5] J.M. Chung and E. Peacock-Lpez, *Bifurcation diagrams and Turing patterns in a chemical self-replicating reaction-diffusion system with cross diffusion*, J. Chem. Phys. **127** (2007), 174903.

[6] J.M. Chung and E. Peacock-Lpez, *Cross-diffusion in the templator model of chemical self-replication*, Phys. Let. A. **371** (2007), 41-47.

[7] D.L. DeAngelis, R.L. Goldstein and R.V. O'Neill, *A model for trophic interaction*, Ecology. **56** (1975), 881-892.

[8] B. Dubey , B. Das and J. Hussain, *A predator - prey interaction model with self and cross-diffusion*, Ecol. Model. **141** (2001), 67-76.

[9] Y.H. Fan and W.T. Li, *Global asymptotic stability of a ratio-dependent predator prey system with diffusion*, J.Comput.Appl.Math. **188** (2006), 205-227.

[10] M.R. Garvie, *Finite-Difference schemes for reaction diffusion equations modelling predator prey interactions in MATLAB*, Bull.Math.Biol. **69** (2007), 931-956.

[11] C. Jost, O. Arino and R. Arditi, *About deterministic extinction in ratio-dependent predator-prey model*, Bull.Math.Biol. **61** (1999), 19-32.

[12] S.A. Levin, T.M. Powell and J.H. Steele, *Patch Dynamics, Lecture Notes in Biomathematics*, Springer-Verlag, Berlin, 1993.

[13] P.P. Liu and Z. Jin, *Pattern formation of a predator-prey model*, Nonlinear Anal. Hybrid Syst. **3** (2009), 177-183.

[14] Y. Lou and W. M. Ni, *Diffusion vs cross-diffusion: An elliptic approach*, J. Differential Equations. **154** (1999), 157-190 .

[15] E.A. McGehee and E. Peacock-Lpez, *Turing patterns in a modified Lotka Volterra model*, Phys. Lett. A. **342** (2005), 90-98.

[16] A. Morozov, S.Petrovskii and B.L. Li, *Bifurcations and chaos in a predator-prey system with the allee effect*, Proc. R. Soc. Lond. B **271** (2004), 1407-1414.

[17] J.D. Murray, *Mathematical Biology*, Springer-Verlag, Berlin, 1993.

[18] M. Sambath, S. Gnanavel and K. Balachandran, *Stability and Hopf bifurcation of a diffusive predator-prey model with predator saturation and competition*, Anal. Appl. 1-18 (2012) DOI: 10.1080/00036811.2012.742185

[19] J.A. Sherratt, *Turing bifurcations with a temporally varying diffusion coefficient*, J.Math.Biol. **33** (1995), 295-308.

[20] X.K. Sun, H.F. Huo and H. Xiang, *Bifurcation and stability analysis in predator-prey model with a stage-structure for predator*, Nonlinear Dyn. **58** (2009), 497-513.

[21] A.M. Turing, *The chemical basis of morphogenesis*, Philos. Trans. R. Soc. Lond. Ser. B: Biol. Sci. **237** (1952), 37-72.

J. KSIAM Vol.16, No.4, 257–257, 2012
(Retraction Notice)

RETRACTION NOTICE TO ”THE RELATIONSHIP BETWEEN NONCOMMUTATIVE AND LORENTZVIOLATING PARAMETERS IN QUANTUM” [J.KSIAM VOL.16, NO.3, 205-216, 2012]

A. HEIDARI, F. GHORBANI AND M. GHORBANI*

INSTITUTE FOR ADVANCED STUDIES, TEHRAN 14456-63543, IRAN

This article has been retracted at the request of the authors and the Editor-in-Chief.

Reason:

This article has been retracted, please see Journal of Korean Society of Industrial and Applied Mathematics on Article Withdrawal:

http://www.ksiam.org

This article has been retracted at the request of the editor as the authors have plagiarized part of a paper that had already appeared in the Iranian Journal of Physics Research:

`http://ijpr.iut.ac.ir/browse.php?a_code=A-10-1-526&slc_lang=fa&sid=1`

One of the conditions of submission of a paper for publication is that authors declare explicitly that their work is original and has not appeared in a publication elsewhere. Re-use of any data should be appropriately cited. As such this article represents a severe abuse of the scientific publishing system. The scientific community takes a very strong view on this matter and we apologize to readers of the journal that this was not detected during the submission process.

*Corresponding author.